

Proposal to upgrade the MIPP Data Acquisition system

D. Isenhower, M. Sadler, R. Towell, S. Watson

*Abilene Christian University**

R. J. Peterson

University of Colorado, Boulder

W. Baker, D. Carey, C. Johnstone, M. Kostin, H. Meyer, R. Raja

Fermi National Accelerator Laboratory

G. Feldman, A. Lebedev, S. Seun

Harvard University

P. Hanlet, O. Kamaev, D. Kaplan, H. Rubin, N. Solomey

Illinois Institute of Technology

U. Akgun, G. Aydin, F. Duru, E. Gulmez, Y. Gunaydin, Y. Onel, A. Penzo

University of Iowa

N. Graf, M. Messier, J. Paley

Indiana University

D. M. Manley

*Kent State University**

P. D. Barnes, Jr. , E. Hartouni, M. Heffner, J. Klay, D. Lange, R. Soltz, D. Wright

Lawrence Livermore National Laboratory

H. R. Gustafson, M. Longo, H-K. Park, D. Rajaram

University of Michigan

K. Hicks

*University of Ohio**

S. P. Kruglov, I. V. Lopatin, N. G. Kozlenko, A. A. Kulbardis,

D. V. Nowinsky, A. K. Radkov, V. V. Sumachev
Petersburg Nuclear Physics Institute, Gatchina, Russia *

A. Bujak, L. Gutay, D. E. Miller
Purdue University

T. Bergfeld, A. Godley, S. R. Mishra, C. Rosenfeld, K. Wu
University of South Carolina

C. Dukes, C. Materniak, K. Nelson, A. Norman
University of Virginia

(Dated: March 29, 2005)

Abstract

The MIPP TPC is the largest contributor to the MIPP event size by far. Its readout system and electronics were designed in the 1990's and limit it to a readout rate of 60 Hz in simple events and ≈ 20 Hz in complicated events. With the readout chips designed for the ALICE collaboration at the LHC, we propose a low cost effective scheme of upgrading the MIPP data acquisition speed to 3000 Hz.

* New MIPP Collaborating Institution

Contents

I. Synopsis	4
II. The proposal to upgrade our data acquisition speed	6
III. Summary of the proposed physics for the current MIPP run	7
A. Scaling Law of Hadronic Fragmentation	8
B. Heavy Ion Physics	11
C. The need to measure particle production from the NUMI target	17
IV. Additional Physics that can be done with the upgraded MIPP	19
A. Non-perturbative QCD	20
B. Ability to measure particle production off more nuclei	22
C. Future Neutrino experiments	22
D. Low momentum pion and kaon physics	22
V. Baryon Spectroscopy with the upgraded MIPP	23
VI. Nonstrange Baryon Spectroscopy	25
A. πN Elastic Scattering	25
B. Single Pion Production	25
C. Strangeness Production	27
D. New Baryons in the $\eta\Delta$ and $\omega\Delta$ Channels	30
E. Beam Time Request For Nonstrange Spectroscopy	32
VII. Pentaquarks	33
VIII. Cascades	34
IX. Details of the TPC DAQ Upgrade	37
X. Brief Description of the MIPP TPC	38
A. ALICE ASICs	40
XI. Data Compression	46

XII. Upgrading the rest of the MIPP DAQ to run at 3 kHz	46
A. Electromagnetic Calorimeter	47
B. Proportional Chambers	47
C. Multicell Cerenkov	47
D. The Time of Flight system	48
E. Drift chambers	48
F. Data Acquisition System Software	48
XIII. Cost and work breakdown of the TPC electronics upgrade	49
A. Optional upgrades	49
XIV. Running time needed for the proposed physics for the upgraded MIPP	49
XV. Conclusions	50
References	50

I. SYNOPSIS

The MIPP experiment ended its engineering run in August 2004 and after the shutdown commenced on its physics run in December 2005. The experiment has since taken physics quality data with both nuclear and cryogenic targets. On 10th November 2004, MIPP was subject to a director's review which came out with excellent reviews on the experiment's readiness and ability to take and analyze data. A prioritized run plan was presented and adopted at the review which is shown in table I. The MIPP run plan is split into three priorities. Data will be taken at different beam momenta on various targets. Priority I data taking will be completed first, followed by priority II and so on. The total data for all three priorities adds to 78.4 million events. The distribution of the required events over targets and beam momenta is shown in table I. The complete MIPP data set is intended to study non-perturbative QCD (Liquid hydrogen data), proton nucleus physics and proton radiography (Be,C,Bi,U,Cu), NUMI target particle production (Thin C, NUMI Target) and atmospheric neutrinos (Liquid Nitrogen). For a detailed description of MIPP physics goals see our proposal [1]. A schematic of the MIPP experiment is shown in Figure 1.

MIPP

Main Injector Particle Production Experiment (FNAL-E907)

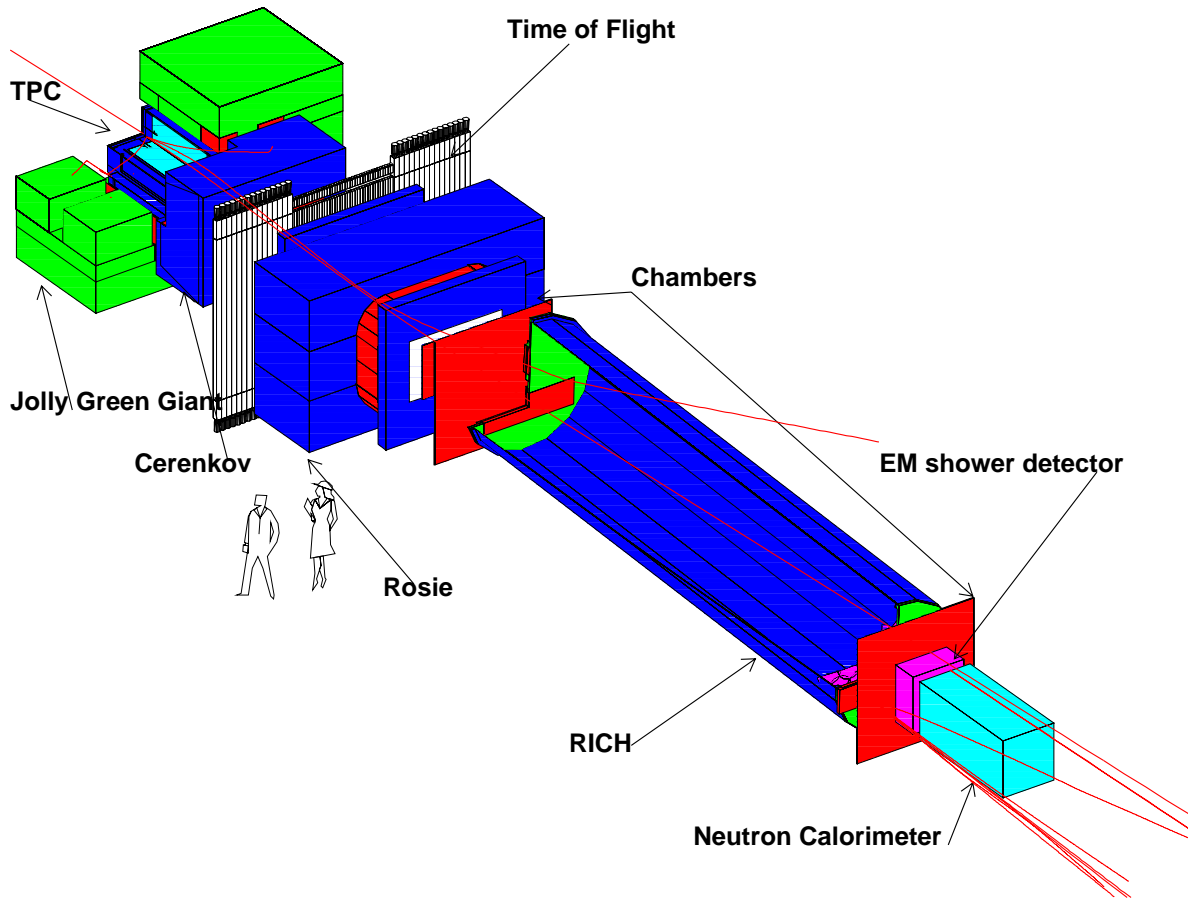


FIG. 1: Schematic of the MIPP detector

Currently we are in the Priority I phase. Physics data taking commenced in earnest on 17th January 2005. From 17th January to 22nd March, when these statistics were tabulated, we have had 295,571 spills of 0.6 seconds flattop delivered in which 272,181 spills had beam. These numbers translate to 13.3 events per spill or a data taking rate of 22 Hz. On average we recorded 45,440 interactions per day. The average rate of beam delivery to MIPP was 6.577 spills per minute (with 6.057 spills per minute with beam). During this period, a calendar time of 64 days, MIPP was live for 31 days and 5 hours. This duty factor was largely due to frequent shots to the Tevatron and also due to transfer of the anti-proton stack to the recycler, the remainder (a few days) due to the time needed to install the cryotarget, beam

studies and detector problems. To date, we have accumulated 3.63 million events.

The introduction of the “double batch” slow spill with a slipstacked high intensity booster batch for anti-protons along with a low intensity slow-spill batch for MIPP and the test beam in late 2004 has permitted the progress we have made to date in obtaining slow spills while the anti-proton stacking was proceeding.

The turn on of the high intensity running of the MINOS experiment and a strict implementation of the 5% rule to cover both MINOS and Tevatron running [2] would imply that the SY120 program will transfer over to one 4-second slow spill every two minutes. Under this scenario, MIPP average data taking will fall to half the current rate and MIPP will accumulate 7.8 million events total (an additional 4.9 million events) during this running period, currently scheduled to end in October 2005.

II. THE PROPOSAL TO UPGRADE OUR DATA ACQUISITION SPEED

The MIPP detector with the largest data output is our TPC. It is also the slowest in outputting this data, since its data acquisition electronics were designed and built [6] in the early 1990’s. The TPC runs at 60Hz for very simple events (single beam tracks). For complicated events this rate currently falls to 20Hz. With modern electronics, it is possible to increase the DAQ rate to 3000Hz, resulting in an over-all increase of 150 in our data acquisition capability. We propose to use the ALTRO/PASA chips designed and thoroughly tested for the ALICE collaboration at the LHC [7]. This technology is also being used for the STAR, BONUS and TOTEM experiments and a large production run is scheduled for May 2005. If MIPP were to get in on this run, the total cost to MIPP to procure these chips (1100 of them) would be \approx \$100,000.

In the scheme outlined below, we propose to acquire these chips in May, design and fabricate our front end electronics cards for the TPC in parallel with our current running. We should then be able return with an upgraded DAQ system in early 2006, when the shutdown (currently scheduled in October) ends. With one 4-second slow spill every two minutes and allowing for a machine duty factor of 50%, we can accumulate 4.32 Million events per day. The entire MIPP run I statistics can be obtained in 18.1 calendar days!

This proposed DAQ capability along with MIPP’s unprecedented acceptance and particle ID abilities has attracted a wider community of users and several new institutions interested

in low momentum (under 5 GeV/c beam momentum) pion and kaon physics have signed this proposal. Other groups have expressed strong interest but could not sign the proposal at this point in time due to contractual obligations.

III. SUMMARY OF THE PROPOSED PHYSICS FOR THE CURRENT MIPP RUN

It behooves us to remind the PAC, the approved physics topics in MIPP that form part of the ongoing run. As detailed in table I, we plan to acquire 78.4 million events over a variety of targets for the following physics reasons.

- To re-open the study of non-perturbative QCD by obtaining high quality data on liquid hydrogen with full particle identification in the final state. The quality of existing data is poor and very often data from different experiments are inconsistent. We plan to test a scaling law of particle fragmentation [3] in 36 reactions to high accuracy.
- To acquire data on various nuclei for the study of proton nucleus interactions and their connection to the quark-gluon plasma question.
- To study nuclear physics scaling behavior.
- To acquire data on nuclei for the investigation of parameters related to proton radiography.
- To improve our model of particle showers in the atmosphere by measuring pion and proton cross sections on nitrogen in order to reduce the systematics in the prediction of the atmospheric neutrino flux.
- To improve implementation of hadronic shower models in programs such as GEANT4, MARS etc by acquiring particle interactions on various nuclei.
- To make our data in DST form on DVD's for others who might be interested in testing various theoretical models.
- To measure the particle production on the NUMI target in detail to predict the neutrino fluxes in the near and far detectors of the MINOS experiment, helping control

the systematics in their measurement of the neutrino oscillation parameters. This data will also be useful for the NOVA and MINERVA experiments that use the NUMI beam.

A. Scaling Law of Hadronic Fragmentation

Even though they form more than 90% of the total inelastic cross section, very little is known about the dynamics of minimum bias interactions. The events are of such low Q^2 that perturbative QCD has little predictive power. Several scaling laws, such as KNO scaling and Feynman scaling, have in the past been proposed to explain the dynamics of minimum bias interactions. All of these have been shown to disagree with experiment.

In 1978, a general law of scaling for inclusive reactions was proposed [3]. It was deduced heuristically, from the need to treat charged pions on an equal footing with neutral pions when extracting the annihilation cross sections, by considering the difference between $\bar{p}p$ and pp cross sections. There were two Phys. Rev. D papers [4][3]. The first shows that it is possible to estimate the annihilation component of $\bar{p}p \rightarrow \pi^0$ inclusive reactions by subtracting the corresponding $pp \rightarrow \pi^0$ component. However, this method fails for the channels $\bar{p}p \rightarrow \pi^+/\pi^-$ because of the different CP symmetry of the corresponding pp component. The situation is remedied by postulating a new equation involving charge asymmetry in $\bar{p}p$ annihilation and non-annihilation components. The new equation lets us extract annihilation information for charged as well as neutral pions by comparing $\bar{p}p$ and pp reactions. These equations were shown to work for 12 GeV/c annihilation reactions.

The scaling law in question was proposed in order to explain the physics behind the asymmetry equation. It states that the ratio of a semi-inclusive cross section to an inclusive cross section involving the same particles is a function only of the missing mass squared (M^2) of the system and not of the other two Mandelstam variables s and t , the center of mass energy squared and the momentum transfer squared, respectively.

Stated mathematically, the ratio

$$\frac{f_{subset}(a + b \rightarrow c + X)}{f(a + b \rightarrow c + X)} \equiv \frac{f_{subset}(M^2, s, t)}{f(M^2, s, t)} = \beta_{subset}(M^2) \quad (1)$$

i.e., a ratio of two functions of three variables is only a function of one of them. When

the subset being considered is annihilations, the asymmetry equation derived in [4] results. The physics behind the scaling law may be understood [3] by considering inclusive cross sections as the analytic continuations of crossed three body interactions, which factorize into a production term that results in the formation of a shortlived fireball of mass M^2 , which subsequently decays into the subset in question. The formation is governed by s and t . The decay term is only a function of M^2 . It should be noted that the physics in question falls outside the scope of perturbative QCD and as such the scaling law is not currently derivable from QCD considerations.

The law was verified in 100 GeV $\bar{p}p$ interactions by considering multiplicity subsets of the reaction $\bar{p}p \rightarrow \pi + X$. It was possible to verify the t independence of the ratio β_{subset} for a variety of subsets with an excellent degree of accuracy. The paper [3] also establishes the s independence of β_{subset} for a variety of $pp \rightarrow p + X$ reactions in the beam energy range of 200–400 GeV/ c . Again, good agreement was obtained between the predictions of the law and data. The law has also been verified in 12 reactions using data from the European Hybrid Spectrometer[8] with various beam particles and final states. Figures 2 and 3 show the test of the law for the reaction $pp \rightarrow \pi^+ + X$ for 400 GeV/ c proton beam for 4 multiplicity subsets: 4-6 prongs, 8 prongs, 10-12 prongs and >12 prongs. Figure 2 shows the agreement between the predictions of the scaling law and subset data as a function of M^2 for various t ranges. Figure 3 shows the agreement between the predictions of the scaling law and subset data as a function of t for various M^2 ranges. The agreement between the predictions of the scaling law and data is excellent in the data tested so far. If the law is an exact one, as there is reason to believe it may be, then it is clearly of fundamental importance in understanding hadronic fragmentation.

The problem with existing data is that it is usually sparse as bubble chambers were being used. *It is very difficult to test the law using existing data for s independence, since only rarely has the same apparatus been used to study the same reaction at multiple energies.*

We propose to measure particle production off hydrogen and other targets as a function of beam energy for various secondary beams ($\pi^\pm, K^\pm, p, \bar{p}$), for a variety of beam momenta ranging from 5 GeV/ c to 85 GeV/ c . At each beam momentum, the data taking rate has to be such that approximately a million unbiased events are recorded for analysis. We plan to test the scaling in 36 reactions. The 36 reactions are with a and c being any of 6 particle species $\pi^+, K^+, p, \pi^-, K^-, \bar{p}$.

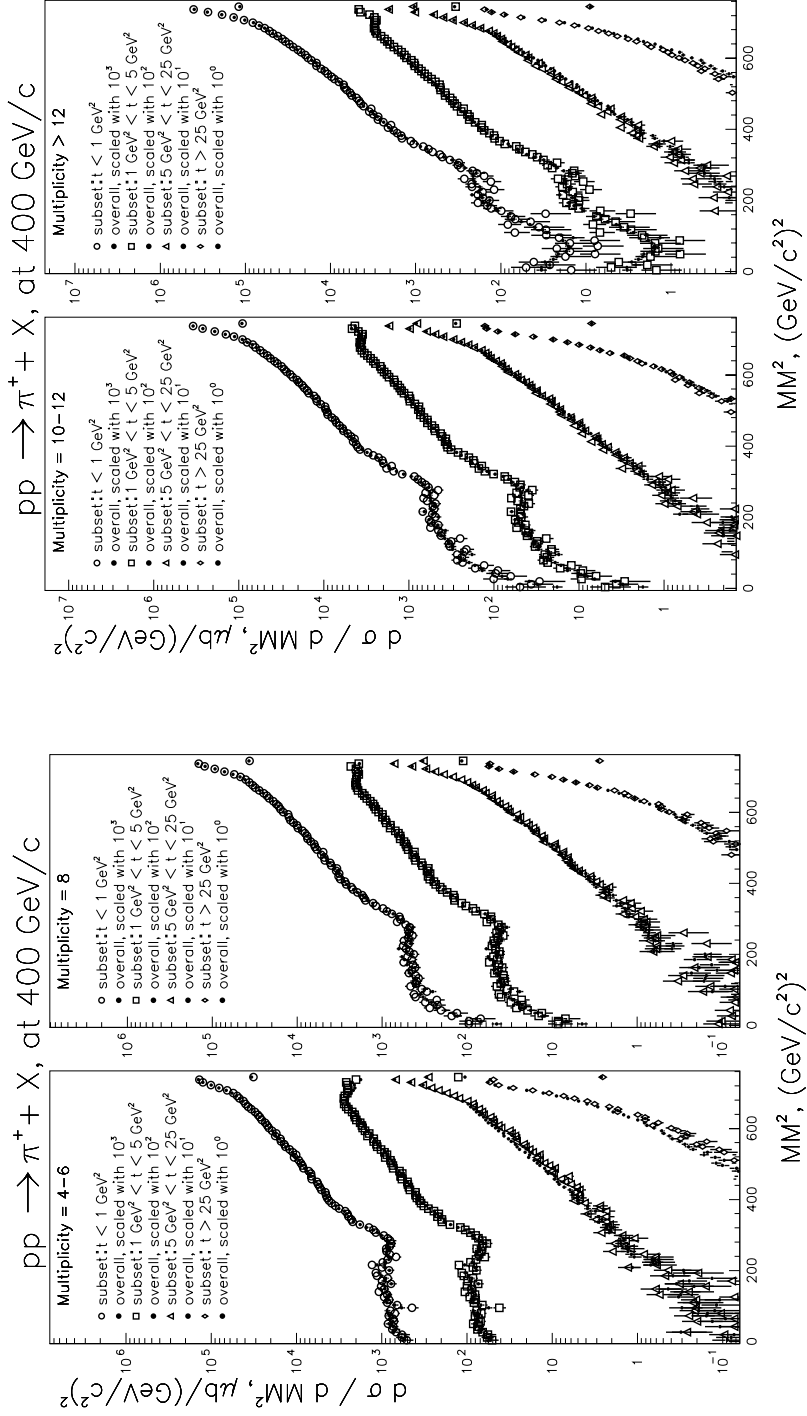


FIG. 2: M^2 distribution for the various subsets in various t ranges. Overall data, weighted by appropriate $\beta_{subset}(M^2)$ is superimposed on the subset data. Data for each t range is offset from the neighboring one by a factor of 10.

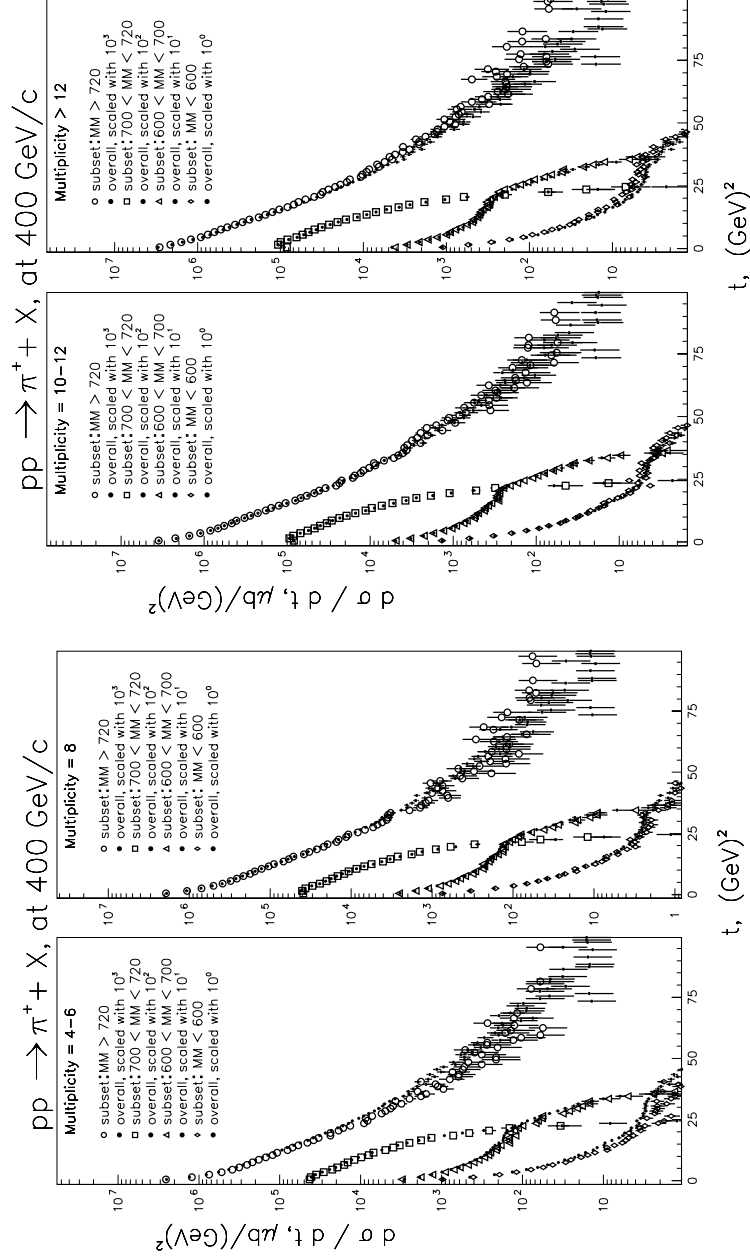


FIG. 3: t distribution for the various subsets in various M^2 ranges. Overall data, weighted by appropriate $\beta_{subset}(M^2)$ is superimposed on the subset data. Data for each M^2 range is offset from the neighboring one by a factor of 10.

B. Heavy Ion Physics

By measuring Λ , Ξ , and Ω production in proton-nucleus collisions as function of the average number of inelastic collisions of the incident proton, MIPP will be able to address a measurement of enhanced strange and multi-strange baryon production in 158 A·GeV/c Pb+Pb

collisions at the SPS. These data will improve understanding of the mechanisms for strangeness production in nuclear (and hadronic) collisions and will test predictions of a phenomenological model for the baryon structure known as the junction [9, 10]. Finally, future comparisons of results from the proton-nucleus program at RHIC to data from MIPP will play a vital role understanding phenomena that are unique to heavy-ion collisions at RHIC energies.

Discovering and studying the QCD phase transition has been the goal of the relativistic heavy-ion programs at the BNL AGS, CERN SPS, and now RHIC. Such a discovery depends on the experiments' ability to extract a set of final state signatures which would mark the occurrence of a the phase transition. Proton-nucleus collisions play a crucial role in providing a calibration for the predicted signatures, both through direct comparison to nucleus-nucleus data, and as input to phenomenological models for nucleus-nucleus collisions.

By the time RHIC was to be commissioned, the CERN program had produced a set of results that were inconclusive when taken individually, but were intriguing when considered together. In the spring of 1999, CERN issued a press release stating that a new state of matter had been formed in heavy-ion collisions. However, there were and still are significant gaps in comparable pA results for many of the proposed signatures. Two of the more important measurements which constitute evidence for new matter formation in Pb+Pb collisions at CERN are the enhanced yields of strange baryons in CERN-WA97 and the suppression of J/ψ charmonium in NA50. The latter result depends on a parameterization of the nuclear absorption/formation of J/ψ in proton-nucleus collisions, and FNAL E866 (and successor E906) are providing important data for understanding the nucleus-nucleus results.

The WA97 results [11] in Fig. 4 show enhanced yields at mid-rapidity of strange and multi-strange baryons per participant nucleon (N_{wound}). Total charged particle yields at mid-rapidity have been observed to be approximately linear in the number of participants or wounded nucleons [12]. The use of this scaling has its origins in the seminal results of an early proton-nucleus experiment run at FNAL [13] which demonstrated that the total charge particle multiplicities are proportional to ν , the mean nuclear thickness traversed by the projectile in a hadron-nucleus collision. For pA collisions, $N_{wound} = \nu + 1$.

However, enhanced strangeness per wounded nucleon is only a meaningful signature of new physics if it can be shown that a similar enhancement is absent in proton-nucleus

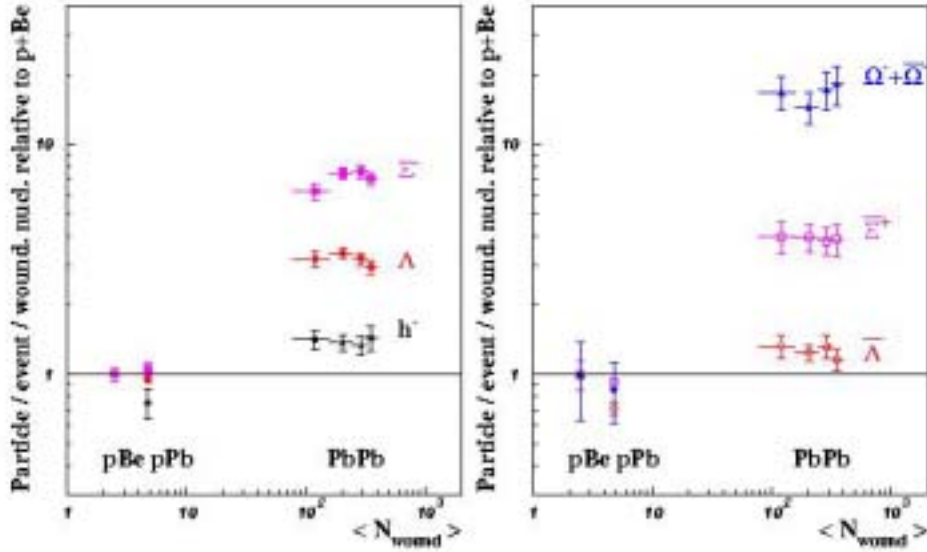


FIG. 4: Hyperon yields per wounded-nucleon in WA97.

collisions. The two data points in Fig. 4 for p+Be and p+Pb are insufficient to make this claim.

The total Λ production in pA collisions has been measured by BNL E910 in 18 A·GeV/cp+Au collisions [14]. Fig. 5 shows Λ yields per event measured vs. the quantity ν or $(N_{wound} - 1)$, measured within the acceptance and extrapolated outside the acceptance. The solid line is the expected wounded nucleon scaling, and the dashed line is the scaling based on the number of collisions. Fig. 5 shows unambiguously that Λ production is enhanced relative to the wounded nucleon scaling. In fact, production initially follows an $N_{collision}$ scaling before saturating after ~ 3 collisions.

It is possible to extrapolate this enhancement in proton-nucleus collisions to heavy-ion collisions by using a parameterization of the pA enhancement as input in a glauber model for heavy-ion collisions. Fig 6 shows the results for such an extrapolation from E910. For the E910 calculation the energy difference is accounted for by a single multiplicative factor which corresponds to the energy dependence measured in pp collisions. Similar results for Λ and Ξ production in 200 GeV/c p+Pb collisions have been reported by NA49 (Fig. 7. In both cases, the remaining enhancement is significantly reduced. Details of these comparisons are discussed in the manuscripts that are in preparation by each collaboration.

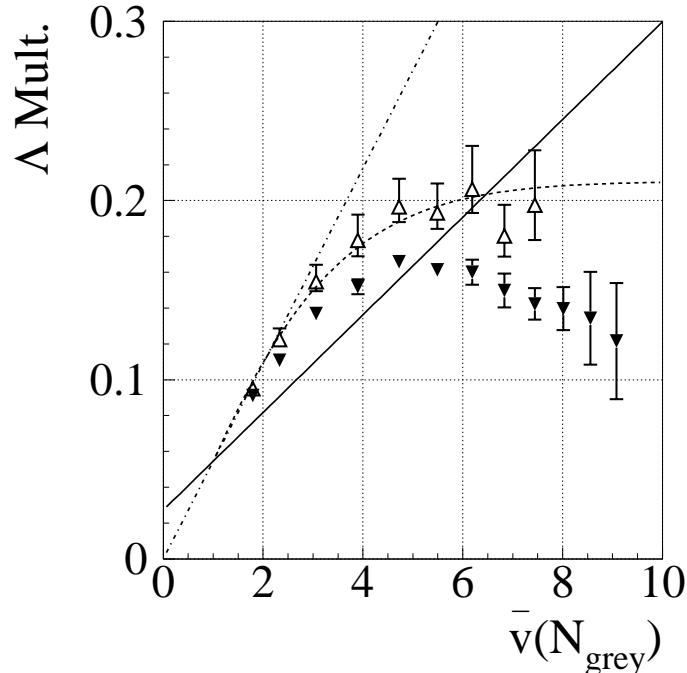


FIG. 5: E910 Lambda yields vs. ν for 18 GeV/c p+Au collisions.

One reason that this result has not been measured earlier is that E910 is the first experiment to combine a high statistics strange particle data set with a simultaneous measure of ν , extracted from the number of target recoil nucleons in the TPC [15]. Using the TPC E910 has been able to identify the top 1% most central events. The NA49 measurement confirms the implications for WA97 but the detector used to measure recoil nucleons had a more limited acceptance for this task; the centrality resolution was less precise. MIPP will combine the high energy data set with the large acceptance for recoil nucleons provided by the TPC. In addition, the expected data sets should yield a measure of Ω vs. N_{wound} .

It has long been thought that the dominant mechanism for exciting and fragmenting the proton in hadronic interactions is the dissociation of one of the valence quarks from the proton through color exchanges with the interacting hadron. Processes that break the diquark or remove all three valence quark from the incoming proton might significantly increase the likelihood of producing singly and multi-strange baryons. In fact, Van Hove [16] in his early model of baryon fragmentation directly related Ξ and Ω production rates to the probability of stripping 2 and 3 quarks from the baryon in a high-energy collision. An

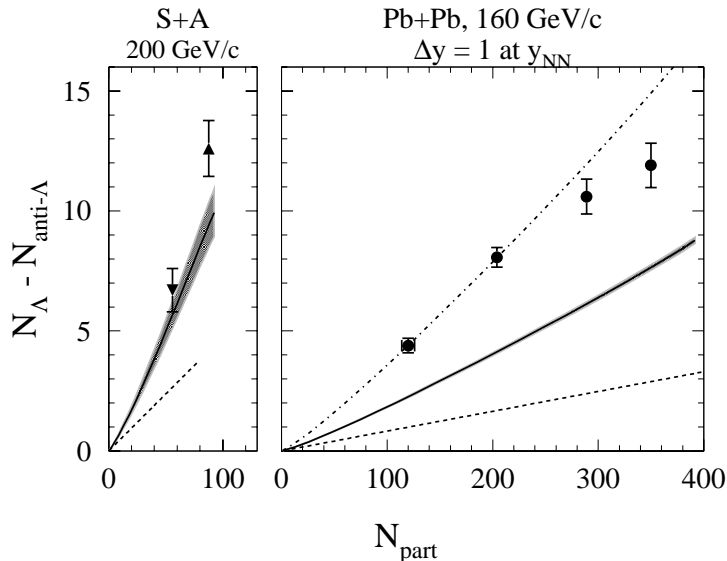


FIG. 6: Extrapolations of E910 proton-nucleus strangeness enhancement to heavy-ion results from WA97. N_{wound} scaling, dashed; E910 extrapolation, solid; Extrapolation with acceptance correction, dot-dashed.

increase in multi-strange baryon production from multiple valence quark stripping processes results simply from the fact that as more valence quarks are stripped, the probability for picking up a strange quark from the sea increases. Considerations of such processes have been spurred by the resurrection of the “baryon junction” originally proposed by Veneziano [9]. The removal of the three valence quarks from a baryon leaves the junction behind and, in the process of becoming color neutral, the associated gluons must pick up replacement quarks out of the sea. Attempts have been made to constrain the parameters of the junction in Regge theory using $\bar{p}p$ annihilation data. Removing the three quarks from the incident proton, processes involving excitation of the junction, may lead to increased strange and multi-strange baryon production [10]. In particular, it will lead to events in which an Omega is produced in association with 3 kaons. While the extraction of the junction may be difficult in interactions in which it is rare (pp collisions), it might be much more likely in proton-nucleus interactions in which the baryon undergoes multiple nucleon-nucleon scatterings.

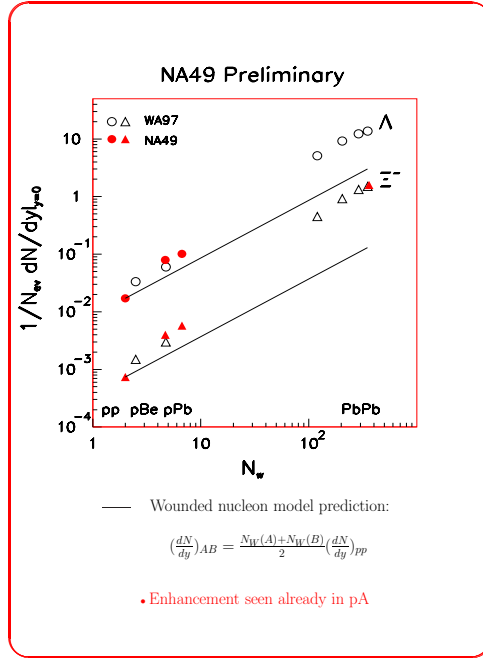


FIG. 7: Comparison of results from NA49 and WA97 reported at Quark Matter 2001 Conference.

Measurements from MIPP, however, could provide much tighter constraints on such a model. If the junction mechanism does play a role in proton interactions, MIPP might be the first to show that clearly by the ability to study both the strange baryon and the associated kaons in events where the proton is known to interact multiple times.

Proton-nucleus (or deuteron-nucleus for machine considerations) running is also an important priority for RHIC. One of the challenges will be to understand the relative components of hard processes, largely absent from the SPS, from the soft process, which appear quite similar to data from the SPS. The multiplicity dependence on centrality is well described by a two component fit, a soft component proportional to N_{wound} and a hard component proportional to $N_{collision}$ [17, 18]. Furthermore, suppression of high p_T hadrons in central collisions, the first qualitatively new result from RHIC, underscores the importance of understanding relative hard and soft contributions. Direct comparisons of proton-nucleus data from MIPP and RHIC may play an important role in calculating the relative strengths of these components. An understanding of the energy evolution of proton-nucleus collisions,

from the BNL AGS (E910) through the CERN SPS and FNAL MIPP to RHIC, is essential to the understanding the corresponding evolution in heavy-ion collisions.

C. The need to measure particle production from the NUMI target

We outline here the need to measure the particle production on the NUMI target. The evidence of neutrino oscillations is obtained from the difference in shapes of the energy spectrum of the neutrino charged current events in the far detector and the near detector. The far detector however sees a point NUMI target, whereas the target at the near detector has finite angular dimensions. Put another way, the neutrinos that interact in the near detector come from the decay of a different kinematic mix of pions than those that interact in the far detector. It is thus important to measure the dynamics of pion production off the NUMI target.

Figure 8 shows the distribution in longitudinal and transverse pions weighted by their contribution to the neutrino event rate in the far and near MINIOS detectors. These weightings are different in detail. Superimposed on this plot are the existing data on hadron production obtained from mainly single arm spectrometer measurements [19], which explains their discreteness in p, p_T space.

Figure 9 shows the predictions of the absolute neutrino rates in the MINOS near detector using four existing hadron production models [20]. The model predictions differ from the average by as much as 20% as a function of neutrino energy. Figure 10 shows the predictions of the ratio of the far to the near neutrino flux using the same four models. Again, there is considerable uncertainty in the predictions, which increases in the high energy tail of the spectrum. The evidence for oscillations is obtained by normalizing the far detector spectrum to the near detector spectrum ($\approx 10^6$ more events in the near detector). The shapes of the two spectra have to agree in the high energy tail (no oscillations), before one can take seriously the expected deficit due to oscillations (in the low energy part of the spectrum). Figure 11 shows the variation of the percentage error in the far/near detector ratio as a function of the number of events obtained in MIPP off the NUMI target, for neutrino energies (3-4 GeV, low energy part, oscillation deficit) and for neutrino energies (20-22 GeV, high energy tail). It can be seen that one needs $\approx 10^7$ events in MIPP on the NUMI target for this percentage error to drop below 3% in the high energy tail.

Low Energy Beam

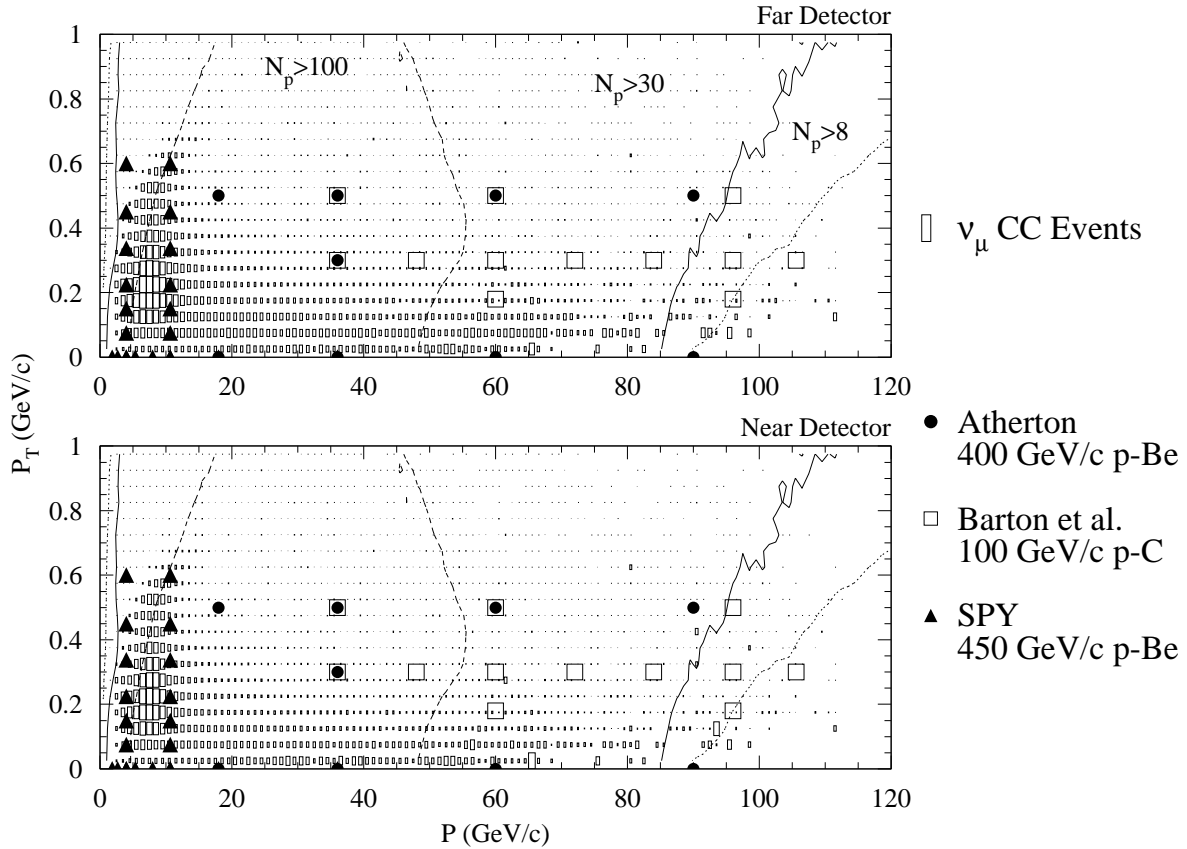


FIG. 8: The distribution in longitudinal and transverse momentum of secondary pions produced on the NUMI target. Secondaries have been weighted by their contribution to the neutrino event rate at the far (top) and the near (bottom) detectors. Overlaid are the locations of existing hadron production measurements

To summarize, MIPP measurements of the NUMI target are crucial to controlling the systematics in the prediction of the far/near ratio of expected events. Understanding this is essential to obtaining precise oscillation parameters. The MIPP measurement will also make the task of understanding the MINOS near detector systematics easier. The experiments NOVA and MINERVA which use the NUMI target also will benefit from the MIPP measurement, as can be seen from their proposals.

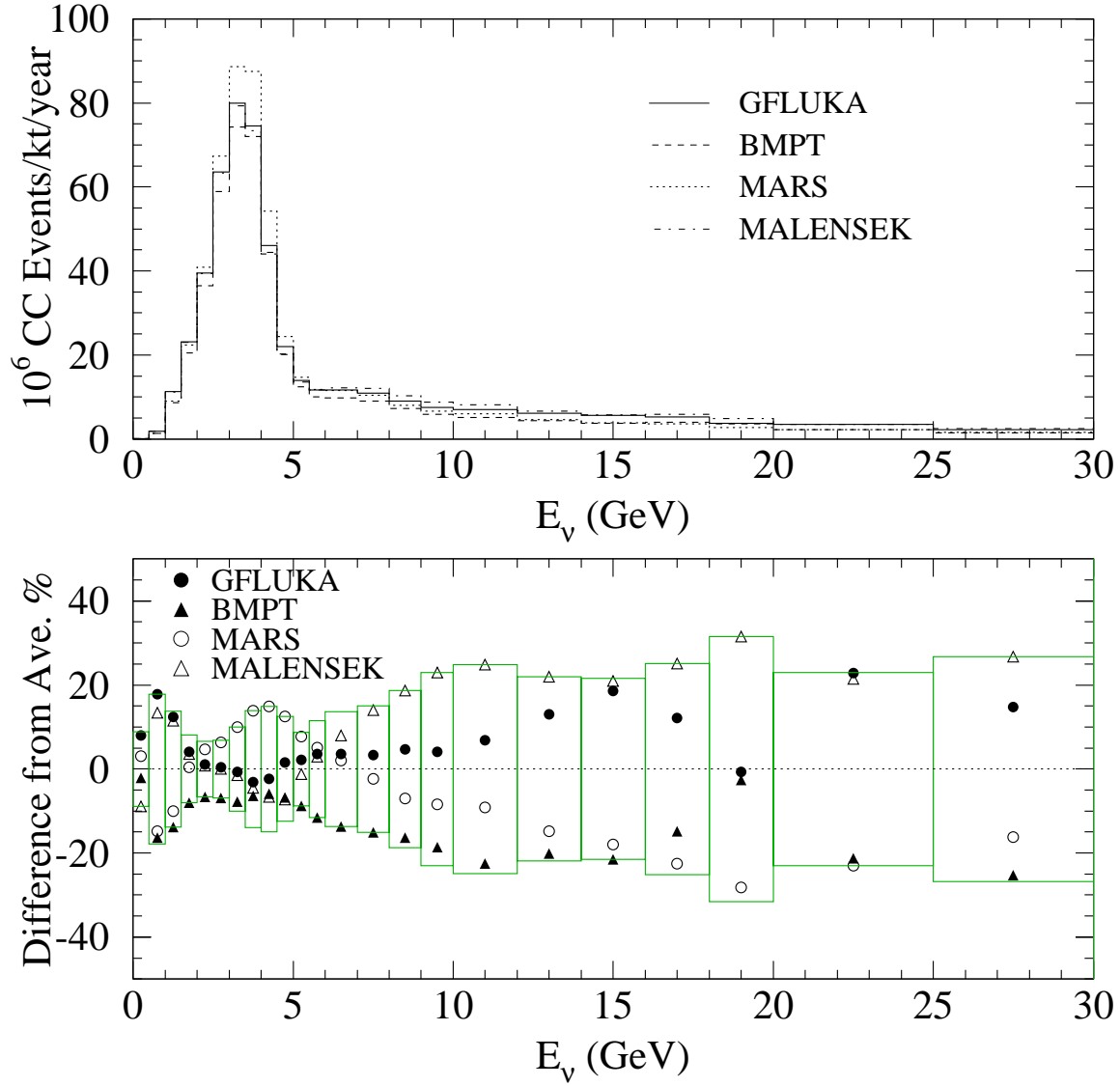


FIG. 9: The predictions of the absolute neutrino rates at the MINOS near detector using various hadron production models.

IV. ADDITIONAL PHYSICS THAT CAN BE DONE WITH THE UPGRADED MIPP

In addition to the physics approved for MIPP I (acquirable in under 20 days), the upgrade extends MIPP's physics capabilities considerably in the following sectors.

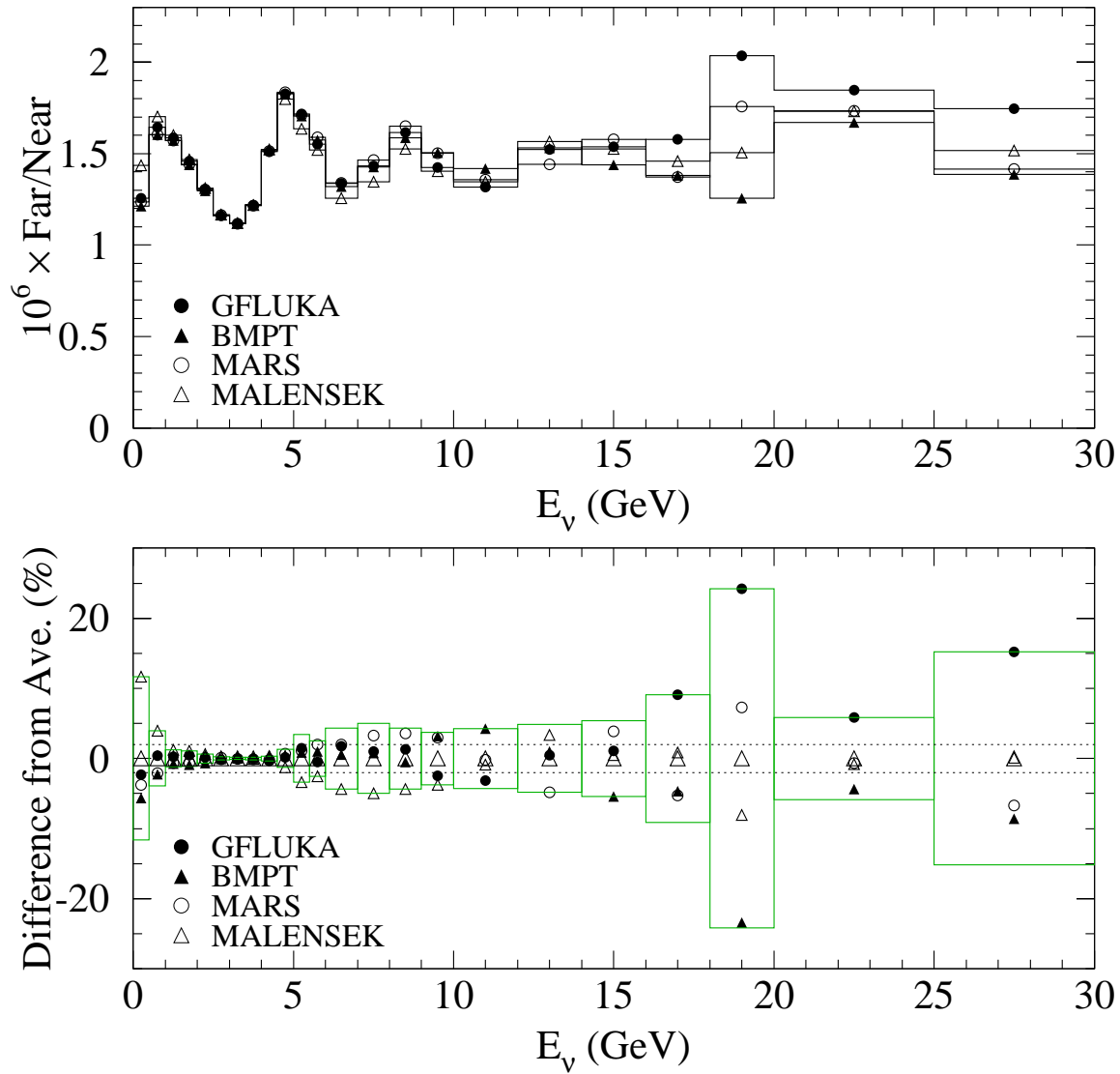


FIG. 10: The predictions for the ratio of the far neutrino flux to the near neutrino flux for various hadron production models.

A. Non-perturbative QCD

If the scaling is found to be obeyed in single particle inclusions, it behooves us to ask whether similar scaling works with two particle inclusive reactions $ab \rightarrow c + d + X$. Testing the scaling in two particle inclusions will require more statistics since there are many more variables to test against. Depending on how well single particle inclusive scaling works, (to

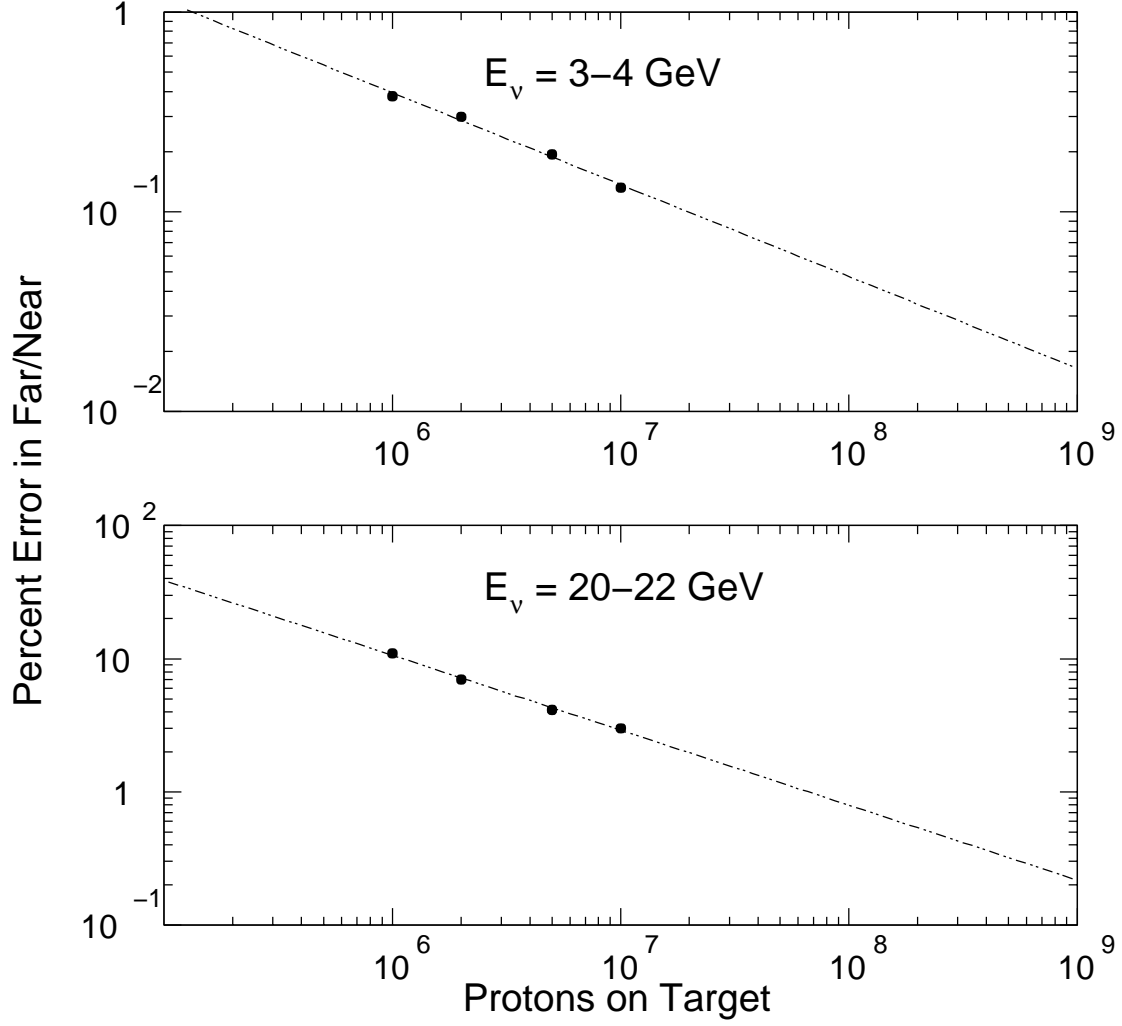


FIG. 11: The percentage error in the far/near ratio as a function of the number of events in MIPP obtained for the NUMI target (labelled protons on target) measurement as a function of the neutrino energy.

be determined with MIPP-I data) we would obtain an event sample of 100 million events (23 days of running) distributed over six beam species and the same beam momenta to test this scaling.

B. Ability to measure particle production off more nuclei

We can extend the MIPP-I data set on the nuclei to other nuclei of interest, e.g. Mercury targets are of interest for neutrino factory. We can indeed obtain measurements over a fair range of the periodic table using six beam species and momenta. Such data sets will be unique and will obviate the need to extrapolate over long ranges in Atomic Weight to predict spectra.

C. Future Neutrino experiments

Proton targets in neutrino experiments (such as the NUMI target currently serving the MINOS experiment) require 10^7 events measured to accurately predict the neutrino flux in the beam line as a function of distance and angle. The NUMI target serves not only the MINOS experiment but also the MINERVA and the NOVA experiments. MIPP measurements will be crucial for all these experiments. The time taken to acquire 10^7 events is 2.3 days. Future neutrino experiments such as FINESSE and T2K can also benefit from this upgrade.

D. Low momentum pion and kaon physics

We have run the MIPP secondary beam line between the momenta 75 GeV/c to 5 GeV/c. The beam line power supplies regulate well down to 5 GeV/c but cannot accurately be controlled below this at present, because the currents become too small. However, we can use trim dipole power supplies (plentiful at Fermilab) below 5 GeV/c [5] and control the beam line well. MIPP would then switch between the two sets of supplies, depending on beam conditions. We can identify the particles in the beam well using our beam Cerenkovs and time of flight. The time of flight will be used for low energy beams. The beam fluxes at our secondary target, taking into account decay in flight, are given in table II.

The present distance from the primary to the secondary target is 95 meters. With no change in beam line design, it is possible to produce a 1 GeV/c pion beam and kaon beams down to 5 GeV/c. With the high DAQ rate of the upgraded MIPP, this permits searches for missing baryon resonances. It also permits us to search for exotic resonances such as pentaquarks or glueballs using six beam species and varying beam momenta. These abilities would make MIPP unique in this field. It can complement the results of photon beam

searches at places such as the Jefferson Laboratory (JLab).

V. BARYON SPECTROSCOPY WITH THE UPGRADED MIPP

Partial-wave analyses of πN scattering data have yielded some of the most reliable information about nonstrange baryon resonances. These analyses provide information about resonance masses and total decay widths (or their pole positions) and πN branching fractions. In order to determine resonance couplings to other channels, it is necessary to study inelastic πN scattering reactions, such as $\pi^- p \rightarrow \eta n$, $\pi^- p \rightarrow \pi^+ \pi^- n$, and $\pi^- p \rightarrow K^0 \Lambda$, to give only a few of many possible examples. Important information is also provided by meson photoproduction experiments, such as $\gamma p \rightarrow \pi^0 p$, $\gamma p \rightarrow K^+ \Lambda$, and $\gamma p \rightarrow \pi^+ \pi^- p$. These hadronic and electromagnetic reactions are all linked by unitarity of the S-matrix, and modern coupled-channel analyses attempt to describe data from both hadronic and electromagnetic channels within a single consistent framework.

The data obtained from πN scattering and meson photoproduction experiments provide crucial information about QCD in the nonperturbative regime. One of the important issues concerns how many internal degrees of freedom are really needed to describe baryon resonances. Essentially all of the known baryon resonances can be described as quark-diquark states, whereas quark models predict a much richer spectrum involving three dynamical quark degrees of freedom. That is, quark models predict many more states than have been observed experimentally. These states are commonly known as “missing resonances”. There are two likely solutions to this puzzle: (1) the missing states simply do not exist; or (2) the missing states have not been seen because they couple weakly to the πN channel. One principal reason for building the CLAS detector at JLab was to look for missing resonances in reactions that do not involve the πN channel. If one were to find evidence for such a resonance in some photoproduction reaction, such as $\gamma p \rightarrow K^+ \Lambda$, then one would like to determine the state’s helicity amplitudes in order to make comparisons with quark-model predictions. This determination, however, is impossible without knowing the resonance’s hadronic coupling to $K \Lambda$, and that cannot be determined without corresponding high-statistics measurements for $\pi N \rightarrow \pi N$ and $\pi N \rightarrow K \Lambda$. Such high-statistics data do not exist.

Because of the limited statistics of data for inelastic πN scattering, essentially every partial-wave analysis (PWA) ever done was an *energy-dependent* PWA. That is, a particular

energy-dependent parameterization was assumed for the partial-wave amplitudes. More often than not, the PWAs were also single-channel analyses, which lead to inconsistent determinations of resonance parameters for different reaction channels. Finally, most of the older analyses assumed simple resonance + background forms for the partial-wave T-matrix amplitudes, which is inconsistent with unitarity of the corresponding S-matrix. With high-statistics data, it should be possible to perform modern coupled-channel partial-wave analyses that will address all of these criticisms with older analyses.

Resonances in πN scattering conventionally fall into well-defined regions, based on the mass of the resonance. The first resonance region is dominated by formation of the $P_{33}(1232)$ resonance. The second resonance region is near a c.m. energy of 1.5 GeV and includes contributions from only three resonances: the $P_{11}(1440)$ or Roper resonance, the $D_{13}(1520)$, and the $S_{11}(1535)$ states. The third resonance region is near a c.m. energy of 1.7 GeV and includes contributions from nine established resonances, including $S_{11}(1650)$, $D_{15}(1675)$, $F_{15}(1680)$, $D_{33}(1700)$, $P_{11}(1710)$, $P_{13}(1720)$, $P_{33}(1600)$, $S_{31}(1620)$, and $D_{33}(1700)$.

The fourth resonance region is near a c.m. energy of 1.9 or 2.0 GeV and includes contributions from several resonances in the $N = 2$ band, most importantly, the $F_{37}(1950)$. (The $N = 2$ band is so called because it consists of positive-parity excited states whose wave functions are predominantly $N = 2$ when expanded in a harmonic-oscillator basis.) There are approximately nine “missing” positive-parity resonances in the $N = 2$ band.

Not much is known about resonances above the fourth resonance region. One expects the region near 2.2 GeV to be populated by several negative-parity states forming the $N = 3$ band. There should also be some low-lying $N = 4$ positive-parity states in this mass range. A pion beam with lab momentum of 0.8 GeV/ c corresponds to the c.m. energy 1.56 GeV, which is just above the peak of the second resonance region. A pion beam with lab momentum of 1.0 GeV/ c corresponds to the c.m. energy 1.67 GeV, which is in the middle of the third resonance region. These energies are both higher than could be reached at either LAMPF or TRIUMF; consequently, there is a strong need for high-statistics measurements of πN scattering reactions starting near 0.8 or 1.0 GeV/ c .

VI. NONSTRANGE BARYON SPECTROSCOPY

A. πN Elastic Scattering

There have been almost no new elastic scattering data at energies above the Roper resonance in about three decades. Some of the old data sets are inconsistent with each other. This is the single most important reaction to have precise data if one wants to make a coupled-channel analysis with the precise single pion photoproduction data coming from JLab and other electromagnetic facilities. Once available in the form of differential cross sections (or other observables), the data can readily be included in the SAID database maintained by the GWU data analysis group [21]. The GWU data analysis group would welcome precise new hadronic data in order to update their partial-wave analyses of pion-nucleon scattering and single pion photoproduction.

B. Single Pion Production

The first important inelastic reaction in pion-nucleon scattering is single pion production. With a TPC, one should be able to measure four of the five charge reactions amenable to $\pi^\pm p$ scattering using standard missing mass (MM) techniques:

$$\pi^- p \rightarrow \pi^- \pi^0 p \quad (\text{detect } \pi^0 \text{ by MM})$$

$$\pi^+ p \rightarrow \pi^+ \pi^0 p \quad (\text{detect } \pi^0 \text{ by MM})$$

$$\pi^- p \rightarrow \pi^+ \pi^- n \quad (\text{detect neutron by MM})$$

$$\pi^+ p \rightarrow \pi^+ \pi^+ n \quad (\text{detect neutron by MM})$$

An isobar-model partial-wave analysis of the world's available set of bubble-chamber data for these reactions was performed about 20 years ago [22]. This entire data set consisted only of a little over 241,000 events. The biggest problems in the analysis began at c.m. energies around 1600 MeV, where the number of important partial waves became greater than the data available needed to determine them. As a result, the amplitudes for such quasi-two-body reactions as $\pi N \rightarrow \pi \Delta$ and $\pi N \rightarrow \rho N$ become quite noisy above about 1600 MeV. There is a very strong need to have more data, so that a new isobar model analysis could be performed to determine the $\pi \Delta$ and ρN couplings of N and Δ resonances more precisely. Such an analysis could incorporate, in principle, the new data for $\pi^- p \rightarrow \pi^0 \pi^0 n$, which were measured at BNL by the Crystal Ball Collaboration [23]. Such an analysis could

also, in principle, shine light on the interesting structure recently seen at JLab [24] in the $ep \rightarrow e'p\pi^+\pi^-$ reaction (see below).

In 2003, the CLAS Collaboration reported measurements of the $ep \rightarrow e'p\pi^+\pi^-$ reaction [24]. The experiment was performed at JLab in 1999 using the CEBAF Large Acceptance Spectrometer (CLAS). The data were analyzed using a phenomenological calculation incorporating the available information on the N^* and Δ resonances in the 1.2–2 GeV mass range. Discrepancies between the data around 1.7 GeV and the calculation were observed, so further analysis was carried out by allowing the resonance parameters to vary in a number of ways. (See Fig. 12.) The best fit corresponded to a prominent wave with $J^P = 3/2^+$ (its isospin is indeterminate). This state could be attributed to the established $P_{13}(1720)$ state, but with parameters significantly modified from its PDG values [25], or it could correspond to a new baryon state. This new state, if it exists, would have a rather narrow width, a strong $\pi\Delta$ coupling, and a small ρN coupling.

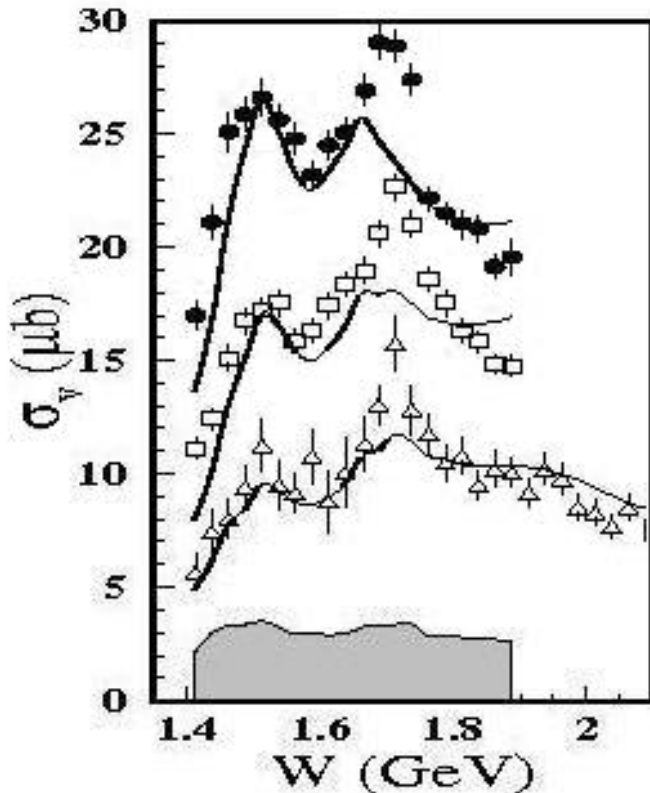


FIG. 12: Total cross section for $\gamma_v p \rightarrow p\pi^+\pi^-$ as a function of c.m. energy W . Data from CLAS are shown at $Q^2 = 0.5\text{--}0.8$ $(\text{GeV}/c)^2$ (full points), $Q^2 = 0.8\text{--}1.1$ $(\text{GeV}/c)^2$ (open squares), and $Q^2 = 1.1\text{--}1.5$ $(\text{GeV}/c)^2$ (open triangles). Error bars are statistical only, while the bottom band shows the systematic error for the lowest Q^2 bin. (Figure taken from Ref. [24].)

C. Strangeness Production

The next important inelastic reaction in pion-nucleon scattering is the η production reaction, $\pi^- p \rightarrow \eta n$. Because of its all-neutral final state, there is no simple way to measure this pure $I = 1/2$ reaction with a TPC. However, we should be able to measure the pure $I = 1/2$ reaction,

$$\pi^- p \rightarrow K^0 \Lambda .$$

The total cross section for this reaction is shown in Fig. 13. The reaction $K^- p \rightarrow K^0 \Lambda$ could be detected from the decays $K^0 \rightarrow K_S^0 \rightarrow \pi^+ \pi^-$ and $\Lambda \rightarrow \pi^- p$. We would therefore look for events of the type $\pi^- p \rightarrow \pi^+ \pi^- \pi^- p$. This is an extremely important reaction to study because it has a sizable cross section and because it is isospin selective. Little is known experimentally about resonances that decay to $K\Lambda$. Of particular interest, we should also be able to determine the final-state Λ polarization, since the Λ is self-analyzing.

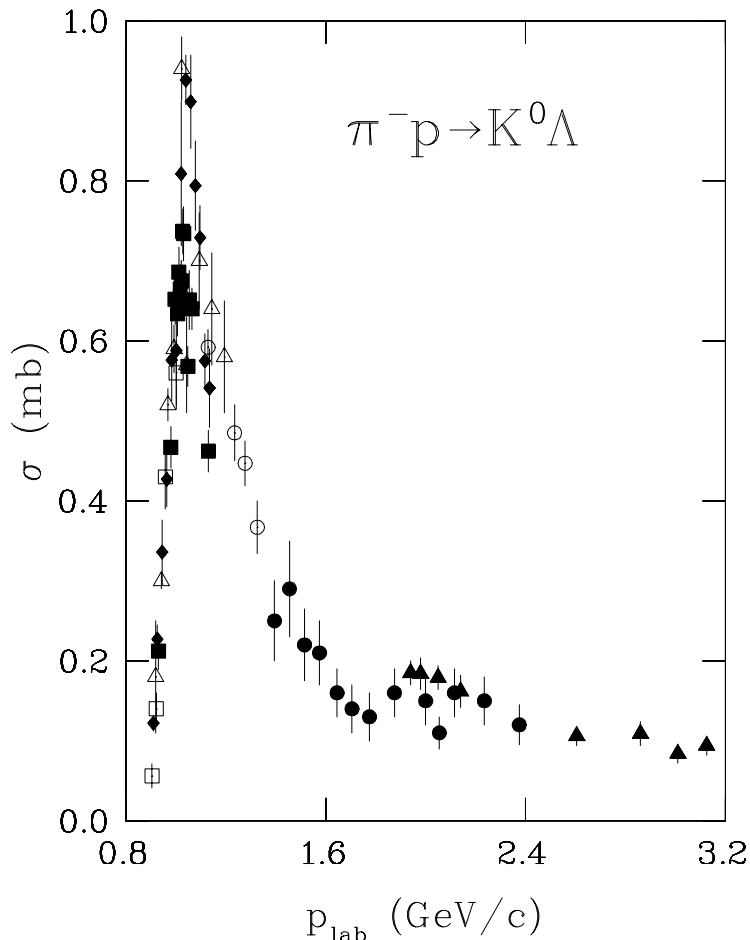


FIG. 13: Total cross section for $\pi^- p \rightarrow K^0 \Lambda$ as a function of laboratory momentum p_{lab} . Data from Bertanza *et al.* [26] are shown as open squares, from Knasel *et al.* [27] as filled squares, from Binford *et al.* [28] as open circles, from Saxon *et al.* [29] as filled circles, from Van Dyke *et al.* [30] as open triangles, from Dahl *et al.* [31] as filled triangles, and from Jones *et al.* [32] as filled diamonds.

Kaon photoproduction data ($\gamma p \rightarrow K^+\Lambda$) measured by the SAPHIR Collaboration from a few years ago caused quite a big stir because of what appeared to be a resonance peak in the cross section near c.m. energy of 1900 MeV [33]. (See Fig. 14.) Quite a few theory papers were written about this structure. For example, one often-cited work proposed that the peak was due to a missing $D_{13}(1960)$ resonance predicted by the quark model [34]. This state might correspond to the two-star $D_{13}(2080)$ listed in the Review of Particle Physics [25].

Recent data from the CLAS collaboration [35] with high statistics and good angular coverage in the region of $W=1.6-2.3$ GeV show that the situation is a bit more complex; the structure near 1.9 GeV is actually two resonances with different masses and angular distributions. In order to understand the underlying resonance contributions, a full coupled channels approach including hadronic rescattering is necessary [36].

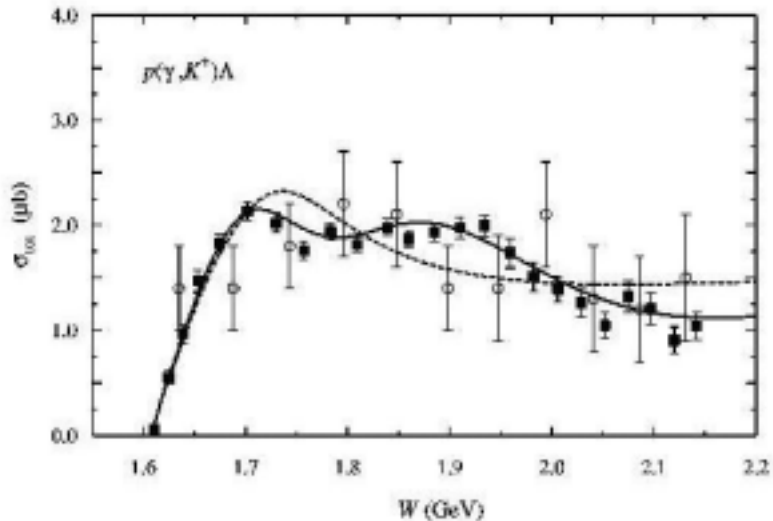


FIG. 14: Total cross section for $K^+\Lambda$ photoproduction on the proton. The dashed line shows the model without the $D_{13}(1960)$ resonance, while the solid line is obtained by including the $D_{13}(1960)$ state. The new SAPHIR data [33] are denoted by the solid squares, old data [37] are shown by open circles. (Figure taken from Ref. [34].)

Precise new $\pi^-p \rightarrow K^0\Lambda$ data would complement the $\gamma p \rightarrow K^+\Lambda$ data and would permit a coupled-channel analysis to be performed for both reactions. Having precise differential cross-section and polarization data for $\pi^-p \rightarrow K^0\Lambda$ should allow a decent partial-wave analysis to be done. Such an analysis should be relatively straightforward to do. The

extracted $K\Lambda$ couplings could be compared with state-of-the-art quark-model predictions, such as those of Capstick and Roberts [38]. With the possible exception of the model state $P_{13}(1950)$, their model predicts that none of the missing positive-parity states in the $N = 2$ band should contribute strongly to $\pi N \rightarrow K\Lambda$. However, these authors predict that a $\pi N \rightarrow K\Lambda$ experiment should show clear signals for several relatively light negative-parity states with wave functions predominantly in the $N = 3$ band. The two-star $D_{13}(2080)$ state should be clearly confirmed with a precision measurement as it should dominate its partial wave. The model state $D_{15}(2080)$ and the nearby weak state $D_{15}(2200)$ should dominate their partial wave in $\pi N \rightarrow K\Lambda$. The weakly established state, $S_{11}(2090)$ should also be visible in this reaction.

We should also be able to make measurements of Σ production by using standard missing mass (MM) and invariant mass (IM) techniques:

$$\pi^- p \rightarrow K^+ \Sigma^- \rightarrow K^+ \pi^- n \text{ (detect neutron by MM; reconstruct } \Sigma^- \text{ by its IM)}$$

$$\pi^+ p \rightarrow K^+ \Sigma^+ \rightarrow K^+ \pi^+ n \text{ (detect neutron by MM; reconstruct } \Sigma^+ \text{ by its IM)}$$

The latter reaction is especially important because it is pure $I = 3/2$ and will excite only Δ^* resonances. In order to perform a proper partial-wave analysis of the first reaction (which is a mixture of $I = 1/2$ and $I = 3/2$), we will also need data for the reaction

$$\pi^- p \rightarrow K^0 \Sigma^0 .$$

This reaction could be detected from the decays $K^0 \rightarrow K_S^0 \rightarrow \pi^+ \pi^-$ and $\Sigma^0 \rightarrow \gamma \Lambda$, followed by $\Lambda \rightarrow \pi^- p$. Thus, one would identify events of the type

$$\pi^- p \rightarrow \gamma + \pi^+ \pi^- \pi^- p .$$

The 77-MeV γ would have to be detected by missing mass and then use invariant mass to reconstruct Λ from $\pi^- p$, and then the Σ^0 from $\gamma \Lambda$.

Resonance couplings determined for $K\Sigma$ could be compared with quark-model calculations, such as those using the relativized quark model of Capstick and Roberts [38]. These authors predict a clear signal for the $N = 2$ band missing positive-parity states $P_{11}(1880)$ and $P_{33}(1985)$ in the reaction $\pi N \rightarrow K\Sigma$. They also predict that the model states $P_{33}(1870)$ and $P_{31}(1835)$ should contribute strongly in this reaction. In addition, several negative-parity states with wave functions predominantly in the $N = 3$ band should contribute strongly to $\pi N \rightarrow K\Sigma$. These include the weakly established states $S_{11}(2090)$, $D_{15}(2200)$, and

$S_{31}(2150)$, as well as the established three-star state $D_{35}(1930)$. A clear signal is predicted for the model states $S_{11}(2030)$ and $D_{15}(2080)$.

Capstick and Roberts have also made quark-model predictions for other channels involving strange particles, such as $K^*\Lambda$, $K\Lambda(1405)$, and $K\Lambda(1520)$. Data for these reactions would be obtained simultaneously with the proposed measurements for $K\Lambda$ and $K\Sigma$.

D. New Baryons in the $\eta\Delta$ and $\omega\Delta$ Channels

The $\eta\Delta$ and $\omega\Delta$ channels are pure $I = 3/2$ and so present an opportunity to search for new and missing Δ^* resonances. The $\eta\Delta$ channel could be studied by the reaction

$$\pi^+p \rightarrow \pi^+\eta p \text{ (identify } \eta \text{ by MM; select } \Delta^{++} \text{ events by IM of } \pi^+p \text{)} .$$

Figure 15 shows a Monte Carlo simulation for the η missing mass in $\pi^+p \rightarrow \eta\Delta^{++}$ at c.m. energy $W = 2.2$ GeV. The simulation includes a total of 50000 events with an assumed 5% signal from $\pi^+p \rightarrow \eta\Delta^{++}$, with 70% background from $\pi^+p \rightarrow \pi^0\pi^0\Delta^{++}$, and 25% background from $\pi^+p \rightarrow \pi^0\pi^0\pi^+p$. A 120-MeV Δ^{++} mass distribution was assumed for both the signal and the background. The simulation shows a clean signal peak for the η meson.

Since the $\eta \rightarrow \pi^+\pi^-\pi^0$ branching fraction is relatively large (22.6 ± 0.4 %), we could also measure this reaction by detecting the π^0 from its missing mass, and then reconstruct the η from its invariant mass in the reaction

$$\pi^+p \rightarrow \pi^+\eta p \rightarrow \pi^0\pi^+\pi^+\pi^-p .$$

The total cross section for $\pi^+p \rightarrow \eta\Delta^{++}$ is shown in Fig. 16.

Similarly, $\omega\Delta$ couplings are also pure $I = 3/2$ and could be studied by the reaction

$$\pi^+p \rightarrow \pi^+\omega p \text{ (identify } \omega \text{ by MM; select } \Delta^{++} \text{ events by IM of } \pi^+p \text{)}$$

The total cross section for $\pi^+p \rightarrow \omega\Delta^{++}$ is shown in Fig. 17. Since the $\omega \rightarrow \pi^+\pi^-\pi^0$ branching fraction is large (89.1 ± 0.7 %), we could also measure this reaction by detecting the π^0 from its missing mass, and then reconstruct the ω from its invariant mass in the reaction

$$\pi^+p \rightarrow \pi^+\omega p \rightarrow \pi^0\pi^+\pi^+\pi^-p .$$

Note that isospin invariance requires

$$\frac{\sigma(\pi^-p \rightarrow \omega\Delta^0)}{\sigma(\pi^+p \rightarrow \omega\Delta^{++})} = \frac{2}{3} ,$$

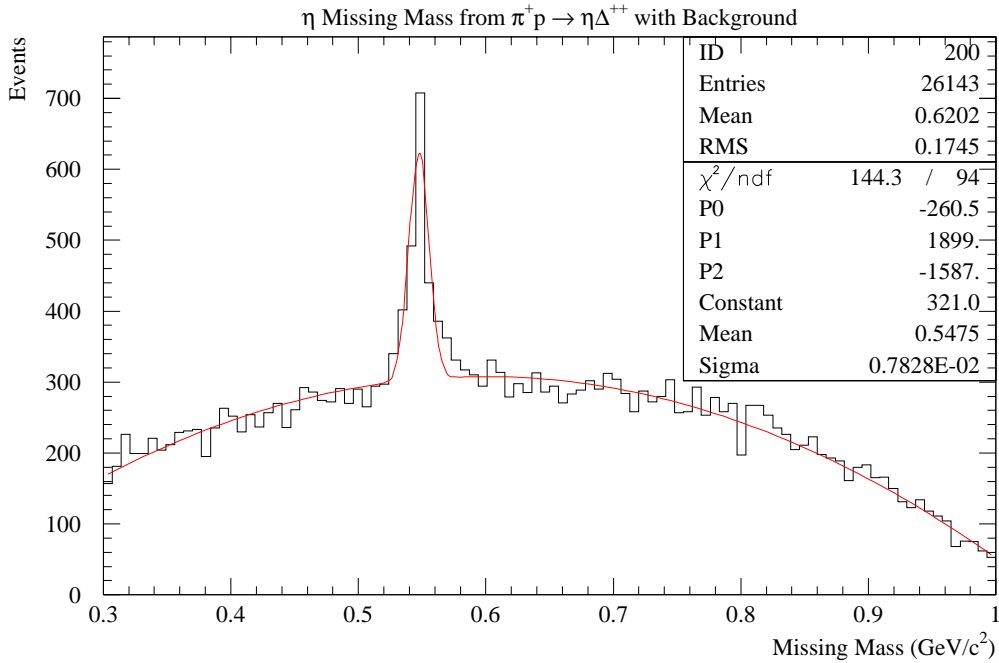


FIG. 15: Monte Carlo simulation of the η missing mass from $\pi^+p \rightarrow \eta\Delta^{++}$ at c.m. energy $W = 2.2$ GeV.

so it is sufficient to make measurements using only π^+ beams.

Quark-model predictions for Δ^* resonances decaying into $\eta\Delta$ and $\omega\Delta$ have been made by Capstick and Roberts [49] using the relativized model of baryon decays based on the 3P_0 pair creation model. Their results show that there should be good signals in $\pi N \rightarrow \eta\Delta$ for the presence of the weakly established first P_{31} baryon, $\Delta(1740)$, the weak second F_{35} state, $\Delta(1990)$, the weak third S_{31} state, $\Delta(2150)$, and the weak second D_{33} state, $\Delta(1940)$. There should also be good signals for two new baryons predicted by their model, namely the missing fourth P_{33} state, $\Delta(1985)$, and a third D_{33} state, $\Delta(2145)$. The same states should also be accessible in $\pi N \rightarrow \omega\Delta$, with the exception of the first P_{31} state, $\Delta(1740)$, and the fourth P_{33} state, $\Delta(1985)$. An experiment to measure $\pi N \rightarrow \omega\Delta$ has the advantage of a higher threshold, so that weakly established or new states are almost always the dominant effects in their partial waves.

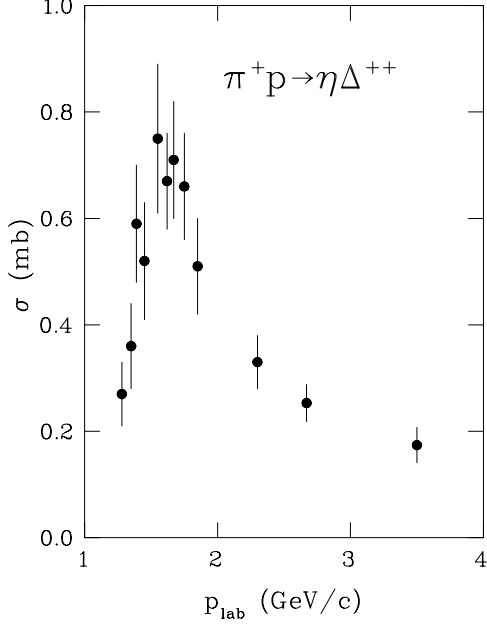


FIG. 16: Total cross section for $\pi^+p \rightarrow \eta\Delta^{++}$ as a function of laboratory momentum p_{lab} . Data from Grether *et al.* [39] are shown as filled circles. Note that isospin symmetry requires $\sigma(\pi^-p \rightarrow \eta\Delta^0) = \frac{2}{3}\sigma(\pi^+p \rightarrow \eta\Delta^{++})$.

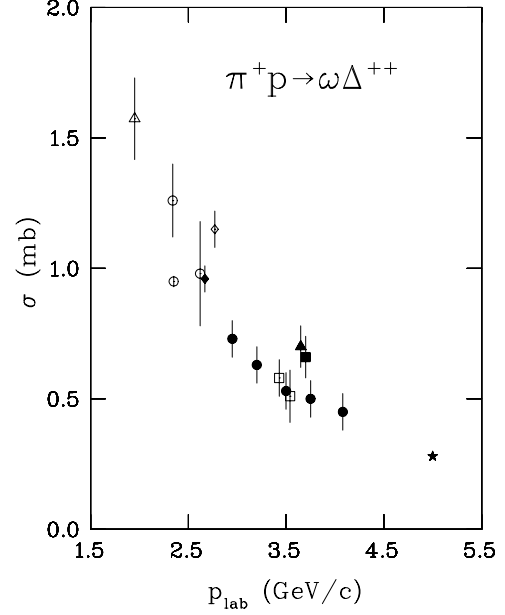


FIG. 17: Total cross section for $\pi^+p \rightarrow \omega\Delta^{++}$ as a function of laboratory momentum p_{lab} . Data from Abolins *et al.* [40] are shown as open squares, from Abrams *et al.* [41] as filled squares, from Alff *et al.* [42] as open circles, from Brown *et al.* [43] as filled circles, from Chapman *et al.* [44] as open triangles, from Trilling *et al.* [45] as filled triangles, from Yamamoto *et al.* [46] as open diamonds, from Buhl *et al.* [47] as filled diamonds, and from Pols *et al.* [48] as a star.

E. Beam Time Request For Nonstrange Spectroscopy

Table III summarizes the beam-time request. For the proposed measurements, we require data with both π^+ and π^- beams in the momentum range 0.8 to 2.5 GeV/ c with momentum bins of about 50 MeV/ c at the lower momenta and 100 MeV/ c at the higher momenta. We request a total beam-time of 1108 hours for π^+ and 876 hours for π^- .

VII. PENTAQUARKS

Concise reviews of the prediction and “discovery” of pentaquarks can be found in the *Review of Particle Physics* [25] and Dzierba, Meyer and Szczepaniak [50]. The latter reference takes a decidedly negative view of the evidence for pentaquarks and should be balanced with other reviews such as Pochodzalla [52] and Hicks [53]. The state discussed here, the $\Theta^+(1540)$, is purportedly a $uudd\bar{s}$ baryon with positive strangeness and zero isospin. The positive results (from LEPs, CLAS and SAPHIR) are from low-energy photon-induced reactions that produce a K^+n mass distribution that peaks in the mass range 1520-1550 MeV/ c^2 . Other positive results (from eight different laboratories!) come from a similar mass peak for K_S^0p , leaving the strangeness ambiguous because of the mixed strangeness of the K_S^0 .

A number of negative results (sixteen are tabulated in ref. [50]) has resulted in considerable skepticism on the existence of the $\Theta^+(1540)$. In general, the negative results have higher statistics and superior resolution and have utilized a variety of production mechanisms, but at higher energy. The positive results have been scrutinized, resulting in criticisms on the handling of backgrounds, possible kinematic reflections enhanced by cuts in the analysis, lack of agreement on the masses reported, and the inexplicably narrow width.

The situation calls for a high-statistics measurement with a K^+ beam to produce this $S=1$ state hadronically. A formation experiment, such as $K^+ + n \rightarrow \Theta^+$ is impractical because of the low momentum (440 MeV/ c) for the K^+ beam. Production experiments, such as $K^+p \rightarrow \pi^+\Theta^+$ and $\pi^-p \rightarrow K^-\Theta^+$, conserve quark flavor and should proceed via the strong interaction. Data for the latter reaction will be produced as a byproduct of the N^* and Δ^* spectroscopy discussed previously using π^- beams at momenta higher than 1.7 GeV/ c . We propose, in addition, an extensive run with a 5 GeV/ c K^+ beam on the 10-cm LH₂ target to search for $K^+p \rightarrow \pi^+\Theta^+$.

Only one of the negative results [51] was a measurement of $K^+p \rightarrow \pi^+\Theta^+$. The experiment used the LASS facility at SLAC with an 11 GeV/ c K^+ beam on an 85-cm LH₂ target and obtained 1 nb⁻¹ of K^+p data. The analysis was done using existing data after publication of the original prediction of the Θ^+ . The prediction of a 10 μ b cross section for $K^+p \rightarrow \pi^+\Theta^+$ was ruled out for a narrow (12 MeV) Θ^+ .

With MIPP, the estimated K^+ rate at 5 GeV/ c is $3.3 \times 10^4 K^+/s$ assuming 2×10^{11} protons/s on the production target. Assuming a 4-second spill every two minutes and a 10-cm

LH₂ target (4.2×10^{-10} protons/nb), we could acquire 0.04 nb^{-1} of K^+p data every day. Thus, 25 days would be required to equal the luminosity of ref. [51], but the acceptance for MIPP is much larger. The authors of ref. [51] expected to see 85 Θ^+ for a cross section of $10 \mu\text{b}$, indicating an acceptance/efficiency combination of 0.85% (given their stated luminosity of 1 nb^{-1}). Our Monte Carlo simulation (assuming an uniform angular distribution in the cm) indicates an acceptance/efficiency of 84%, giving 100 times the sensitivity to the existence of the Θ^+ for the same luminosity. The MIPP situation is further enhanced by the fact that the Θ^+ production cross section at $5 \text{ GeV}/c$ is expected to be larger than at $11 \text{ GeV}/c$ and the backgrounds should be lower. Weighing these considerations, we request 12 days of running for a pentaquark search. We expect a sensitivity approximately two orders of magnitude higher than that obtained in ref. [51].

A Monte Carlo simulation for $K^+p \rightarrow \pi^+\Theta^+$ in MIPP is shown in Fig. 18. The Θ^+ missing mass is reconstructed assuming a 0.5% uncertainty in the incident beam momentum and standard estimates for MIPP resolution depending on the number of pads that are detected. The Θ^+ is presumed to have negligible width (compared to detector resolution), consistent with previous positive results. A background of $K^+p \rightarrow \pi^+K^+n$ (phase space) is included with two different assumptions for the signal-to-background ratio (2% and 0.5%). Simulations were done for incident kaon momenta of $3 \text{ GeV}/c$ and $5 \text{ GeV}/c$.

VIII. CASCADES

As discussed in the nonstrange (S=0) baryon spectroscopy part of this proposal, discovery of the excited states of the nucleon, the N^* 's and the Δ^* 's, has come from partial wave analyses of these states being formed from pion-nucleon scattering. Likewise, strange (S=-1) baryon spectroscopy, the Λ^* 's and Σ^* 's, has relied primarily on direct formation of these states via K^-p scattering, e.g. $K^-p \rightarrow (\Lambda^* \text{ or } \Sigma^*) \rightarrow \text{decay products}$. However, discovery of the excited states of S=-2 baryons, the Ξ^* 's (cascade hyperons), has been obtained primarily from production mechanisms. Production of these states via the $K^-p \rightarrow K^+\Xi^*$ reaction is proposed here for the MIPP upgrade program.

Again, a concise review of the status of our knowledge of Ξ resonances is found in the *Review of Particle Physics* [25]. Quoting, "Not much is known about Ξ resonances. This is because (1) they can only be produced as a part of a final state, so the analysis is more

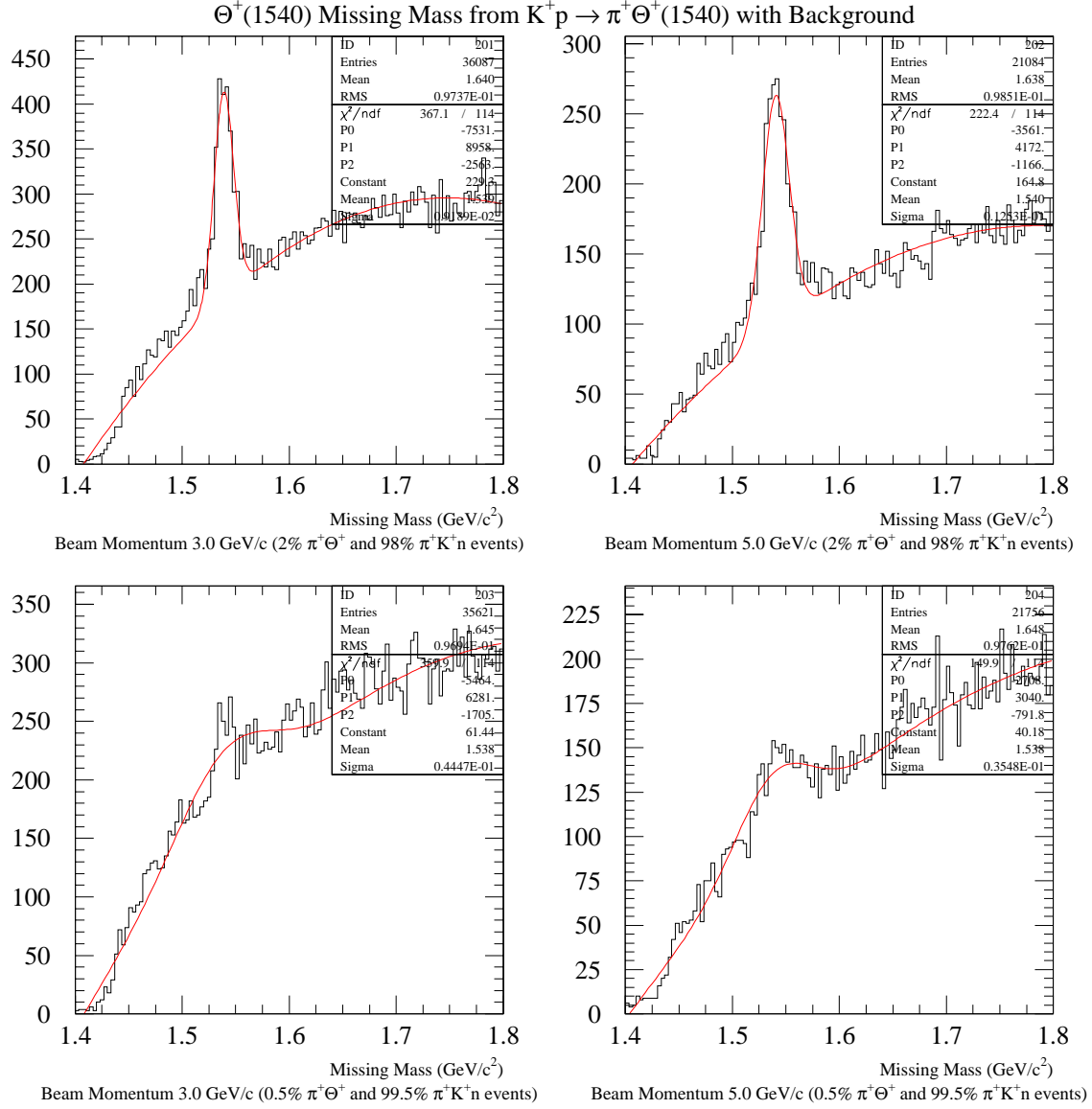


FIG. 18: Monte Carlo simulation of the Θ^+ missing mass from the reaction $K^+p \rightarrow \pi^+\Theta^+$ with incident kaon momenta of 3 and 5 GeV/c. A 0.5% uncertainty in the incident beam momentum is assumed, and standard estimates are made for MIPP resolution depending on the number of pads detected. The Θ^+ is assumed to have negligible width. A background of $K^+p \rightarrow \pi^+K^+n$ is included with signal-to-background ratios of 2% and 0.5%.

complicated than if direct formation were possible, (2) the production cross sections are small (typically a few μb) and (3) the final states are topologically complicated and difficult to

study with electronic techniques. Thus early information about Ξ resonances came entirely from bubble chamber experiments, where the numbers of events are small, and only in the 1980's did electronic experiments make any significant contributions. However, nothing of significance has been added since our 1988 edition.”

By SU(3) flavor symmetry, the spectrum of Ξ^* states has a one-to-one correspondence with N^* and Δ^* states. In the conventional quark model, the N^* 's are radial and rotational excitations of udd and uud configurations and the Ξ^* 's are excitations of uss or dss combinations. Thus, the same question of “hidden” or “missing” resonances appears. Only 11 Ξ 's are listed in Ref. [25] (including the ground state), while 44 are predicted. These states are much narrower than the N^* 's (tens of MeVs rather than hundreds), making them easier to identify and distinguish. Hence, the study of the spectrum of doubly strange hyperons provides advantages in understanding the spectroscopy of all hadrons in particular and nonperturbative QCD in general.

A Monte Carlo simulation, see Fig. 19, indicates that the MIPP beam momentum resolution is a critical factor in resolving these states. Simulated here are the lowest three Ξ 's listed by the PDG [25], assuming their values for the masses and widths. The middle state in Fig. 19, the $\Xi(1620)$, is a one star resonance, meaning that “evidence of existence is poor”. If it exists, it presents a particular problem for quark models because of its low excitation (only 300 MeV above the ground state). In contrast, the first excited N^* state is the Roper resonance at 1440 MeV, 500 MeV above the ground state.

Experiments on photoproduction of Ξ^* 's are underway at Jefferson Laboratory [54, 55] and more are planned as part of the 12-GeV upgrade. Direct production via $K^-p \rightarrow K^+\Xi^*$ should produce these states more copiously and with less background. Ref. [54] reports two structures, at 1770 and 1860 MeV, that are not included in the *Review of Particle Properties* [25]. Enticingly, the NA49 group at CERN has reported a pentaquark candidate at 1862 MeV [56]. Monte Carlo simulations using a 5 GeV/c K^- beam indicate the present MIPP momentum resolution (0.5%) will make it difficult to distinguish these states (if they exist) from the two known states, $\Xi(1820)$ and $\Xi(1950)$.

We request an extended run using a K^- beam at a selected momentum in the 3-5 GeV/c range. The actual beam momentum will be selected based on experience from the present run and continuing Monte Carlo studies. Assuming 5 GeV/c K^- , the beam rate is 70% of the K^+ rate discussed in the previous section for the pentaquark search. A luminosity of 0.4

nb^{-1} would be achieved in 15 days (our request), which would produce 4000 Ξ^{*} 's for each state if the production cross section were $10 \mu\text{b}$.

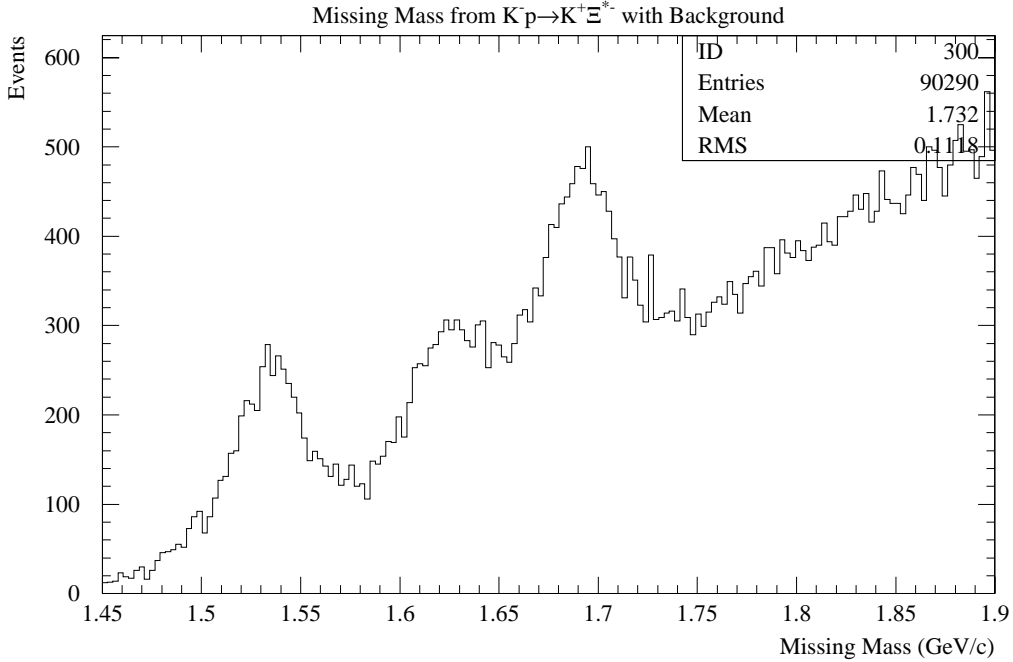


FIG. 19: Monte Carlo simulation of $K^-p \rightarrow K^+\Xi^{*-}$. The simulation includes a total of 100000 events with an assumed 5% signal at each of the three resonances $\Xi(1530)^-$, $\Xi(1620)^-$, and $\Xi(1690)^-$ from $K^-p \rightarrow K^+\Xi^{*-}$. The assumed background is 34% $K^-p \rightarrow K^+K^-\Lambda$, 34% $K^-p \rightarrow K^+\Xi^-\pi^+\pi^-$, and 17% $K^-p \rightarrow K^+\Xi^-\pi^0$. The lab momentum is $3.0 \text{ GeV}/c$. Masses and widths were taken from Ref. [25] estimates. A 0.5% beam momentum uncertainty was assumed, and the momentum resolution of the final state K^+ was estimated by tracking it through the MIPP Monte Carlo, counting the number of pads digitized and applying multiple-scattering and digitization errors.

IX. DETAILS OF THE TPC DAQ UPGRADE

The next production run for the ALICE chips is scheduled in May 2005. If MIPP gets in on that chip order, we can reduce the cost by sharing the overhead with the STAR collaboration as well as the BONUS and TOTEM experiments all of which plan to make use

of the ALICE chips. Work on building the electronics for the upgraded TPC can be carried out in parallel with the on-going MIPP run.

X. BRIEF DESCRIPTION OF THE MIPP TPC

The MIPP TPC [6] was originally designed and used at LBNL in the EOS (E987) experiment and later at BNL (E895). The TPC encompasses an active gaseous volume of 96cm wide by 150cm long by 75cm high (the drift direction), corresponding to a maximum collection time of $15 \mu\text{sec}$. To minimize space charge build up, the TPC incorporates a gating grid (currently limited to a maximum pulse rate of 3kHz) which is pulsed to allow only ionization related in time. Because of limitations in the readout electronics described below the trigger rate is presently limited to about 50Hz. Figure 20 shows a beam's eyeview of the MIPP TPC.



FIG. 20: The MIPP TPC.

The information from the 15,360 channels in the TPC is used to determine with high precision, in three dimensions, charged particle tracks emerging from the target station mounted on the front aperture of the detector. This chamber has the ability to independently records over 3,800,000 individual data points for a single interaction event and forms the basis of the precision momenta and dE/dx measurements for each particle trajectory. The original device that was refurbished for E907 was designed with a readout system that limited the total data acquisition rate to a maximum of 60Hz. Redesign and updating of the TPC front end electronics, replacing the aging 20 year old components with new high density components, is projected to allow a 50 fold increase in the maximum readout rate of the detector to a theoretic limit of 3kHz.

Currently the readout of the TPC is limited by the multiplexed serial readout system which operates on non-zero suppressed data samples for each given event. In this manner the maximum readout speed is limited to 60Hz, due to the high channel count readout and slow (1Mhz) multiplexing/digitization system. The observed occupancy however, for a typical interaction event in the TPC is only on the order of 5% of the total channel count. This results in the possibility of greatly increasing the readout capabilities of the detector by performing the initial data filtering on board the front end electronics and reducing by at least an order of magnitude the data throughput that is currently required for a single system read. The readout can be further enhanced by improving the digitization time required for each pad row and increasing the over all parallelization of the readout system.

The design goal of the proposed electronics upgrade is to bring the speed of the readout system to 3kHz for normal operation of the system. Operation of the system at 3kHz requires that sustained readout of the chamber be accomplished in less than 0.3ms. Non-uniformities in event rate induced by beam structure, restricts this rate in such a manner that the operational time for full event readout should not exceed 0.2ms during burst operation for sustained high speed data acquisition.

The average zero suppressed data size for events as measured during the '04 commissioning run was determined to be on the order of 115kb for multi-track interaction event. The raw data rate when combined with transaction overhead results the requirement that the output data pathway be designed to accommodate a single spill burst data rate of 575mb/s. The proposed upgrade addresses this throughput via a minimum 5-way parallelization of the output data-way, resulting a requirement of only 115mb/s per primary data pathway

which is compatible with commercial data bus implementations.

Upgrade of the TPC front end cards (FECs) to meet these requirements has been studied using a pair of custom designed ASICs that have been engineered, tested and produced for A Large Ion Collider Experiment (ALICE) collaboration at the LHC for use in their more than 570,000 channel time projection chamber. The system incorporates two separate chips, “PASA” an analog preamp/shaper and “ALTRO” a fast ADC/filter which provides event buffering, baseline corrections, signal filtering and zero suppression. The two chips are integrated in a standardized front end card with a dedicated data bus that is synchronized to the main data acquisition system via a series of readout control units (RCUs). The system has also been adopted by the BONUS collaboration for use in their TPC in Hall B of Jefferson Lab, as well as by the TOTEM experiment at CERN.

A. ALICE ASICs

To accommodate the readout of 570,136 charge collection pads, each sampling at a maximum of 1000 samples per event, the ALICE collaboration designed and engineered two custom ASICs to operate in the high rate environment of the LHC heavy ion program. The ALICE readout design, as would be incorporated into the upgrade of the E907 TPC would replace both the analog and digital portions of the current front end electronics cards. Each of the existing 128 analog/digital electronic “sticks” as shown in Fig. X A would be removed and replaced in a one to one manner with an ALICE FEC as shown in Fig. X A, redesigned to match the physical dimensions of the aluminum cold plate upon which the current electronics are mounted. Additionally the cards would be fitted to use zero insertion force (ZIF) socket compatible with the current TPC chamber connections and interlocks. This redesigned FEC follows in all other respects the electrical design and characteristics of the current CERN board layouts.

The ALICE system as shown in Fig. 22 is divided into two stages. The raw signals from the detector pad rows are first fed into a custom designed integrated circuit referred to as “PASA” which serves as the preamp and pulse shaper for each channel[58]. The raw charge collected from the sample window is reshaped into a sharply peaked output distribution of width $\mathcal{O}(190ns)$, as shown in Fig. 23, which is matched to the input requirements of the ALTRO chip for accurate digitization. Each PASA chip services 16 readout pads and is

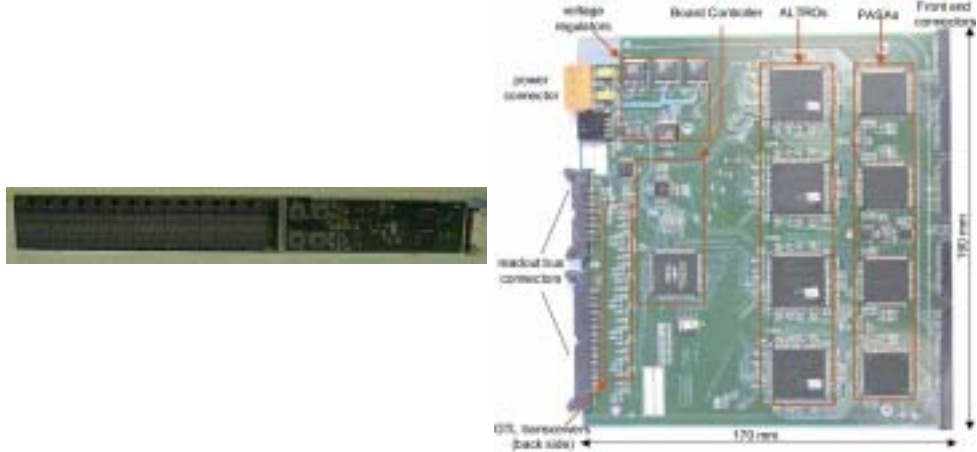


FIG. 21: TPC front end electronics boards for E907 and ALICE. The difference in physical form factor requires a redesign of the ALICE board to match the E907 cold plates and connectors

matched to the ADC inputs of the ALTR0 chips shown schematically in Fig. 24 for a single digitization channel. The ALTR0 ASIC as shown in Fig. 25 is a 16 way parallel system including on each channel a 10MHz ADC, digital signal processor, and memory buffer. The operation of the chip is compatible with normal fixed-target data acquisition operation. Although the signals are sampled continuously the data is processed (pedestal subtraction, shaping and sparsification) only upon receipt of a Level 1 trigger signal. The processed data is stored in the memory buffer upon receipt of a Level 2 accept signal or otherwise discarded. The chips are controlled over a 40bit wide “ALTR0 BUS” developed at CERN [59][60] for communication with with a Readout Control Unit (RCU).

The RCU system, as shown in Fig. 26, serves as the interface between the experimental acquisition and control software and the front end cards. Each RCU is designed to interface with a set of 12 front end cards providing a single high speed data pathway for the zero suppressed event data. The protocol of the output data path is customizable and has been shown to operate both with the high speed serial link protocols developed at CERN, as well as the more common USB protocol and peripheral connection interface (PCI) to bridge the data directly into single board computer memories for further processing. Prototypes of the various RCU interface cards as shown in Fig. 27 and Fig. 28 and have been built and tested both by the ALICE and BONUS collaborations using standard PC based test stands like the one pictured in Fig. 29. The current prototyped RCUs would need no further adaptations

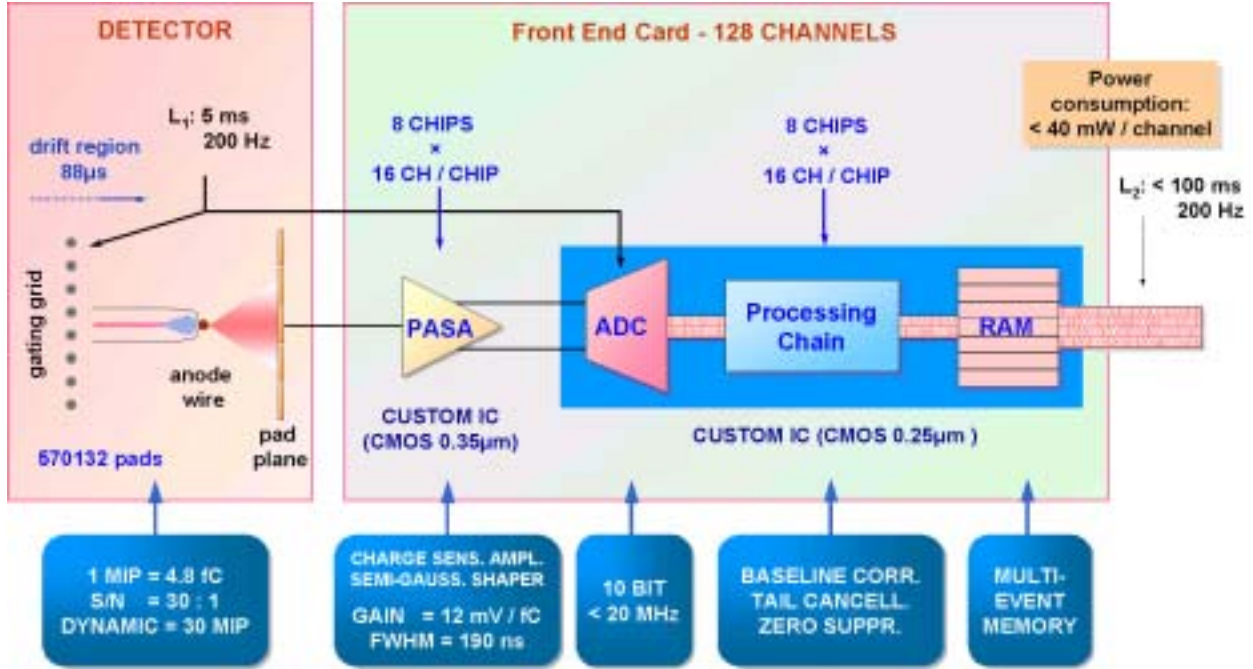


FIG. 22: ALICE front end card and readout system block diagram[60]

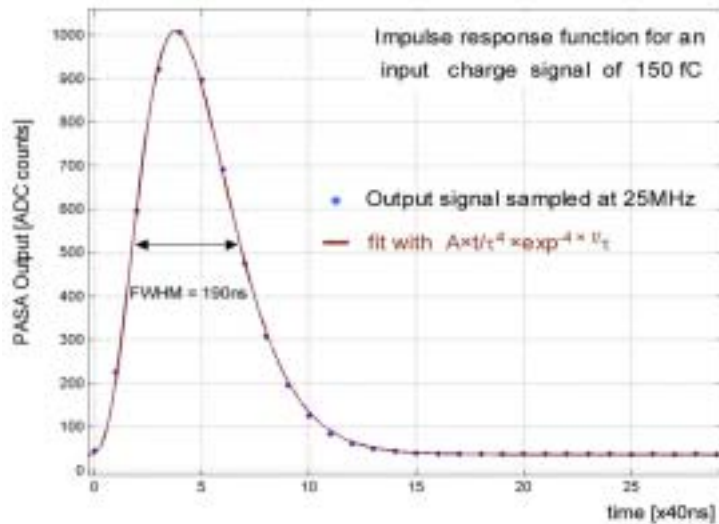


FIG. 23: PASA output function for an initial test charge of 150 fC [61]

to interface directly with the current VME signal board computer system used in the E907 system.

Implementation of the ALICE front end electronics in the E907 TPC require that several additional modifications be made to match the operational needs of the existing hardware.

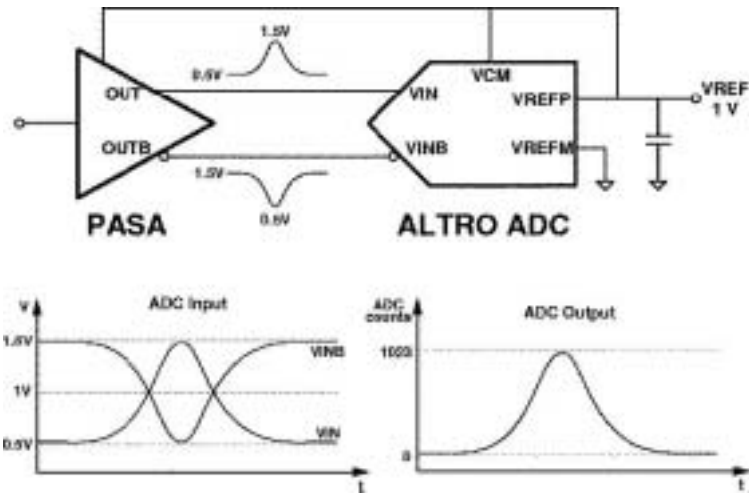


FIG. 24: PASA to ALTRO digitization logic[62]

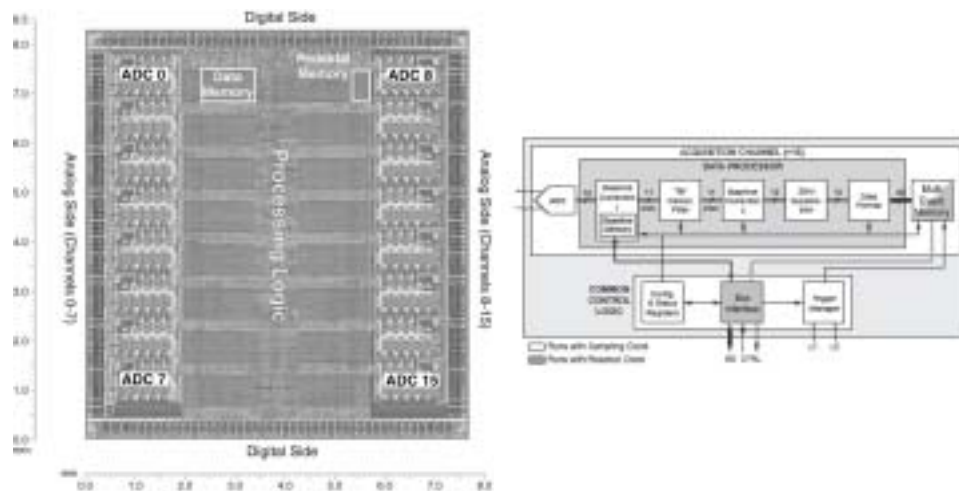


FIG. 25: The ALTRO chip developed at CERN services the readout of 16 channels by integrating a fast ADC, signal processing and event buffering in a single package with interface to a high speed data bus and programming lines

The time window for event scanning and digitization will be reduced from 1000 samples per event to 250 samples to match the drift time over the active volume of the detector. The reduced number of samples then allows for additional segmenting of the ALTRO event buffer in such a manner that the FEC cards will be able to fully buffer 8 events at a once. To ensure that the heat load generated by the new front end boards is compatible with the existing cold plates and water cooling system, provisions have been made to operate the ALTRO

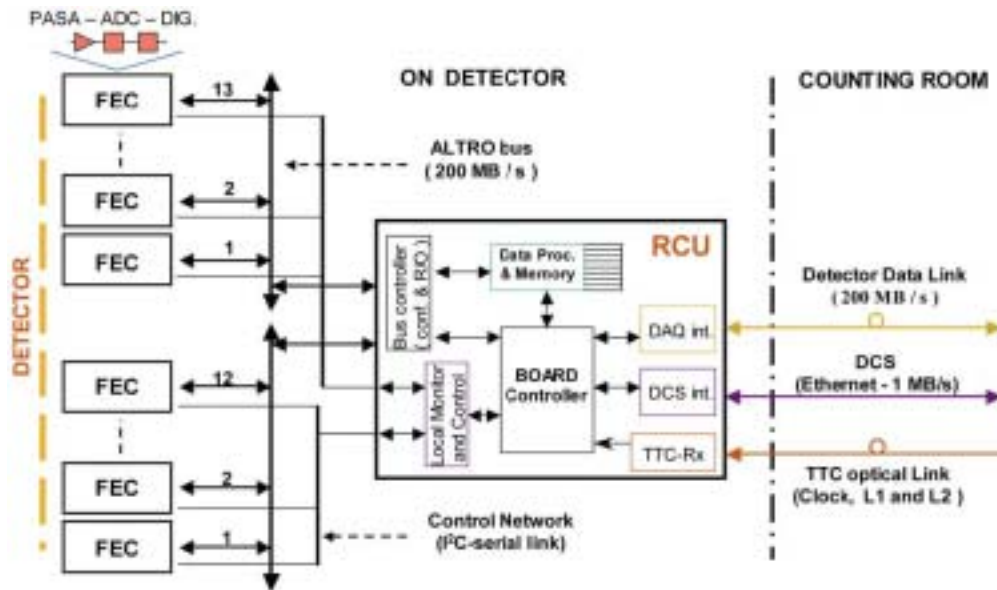


FIG. 26: Readout control unit interface between front end cards and main data acquisition system[63]

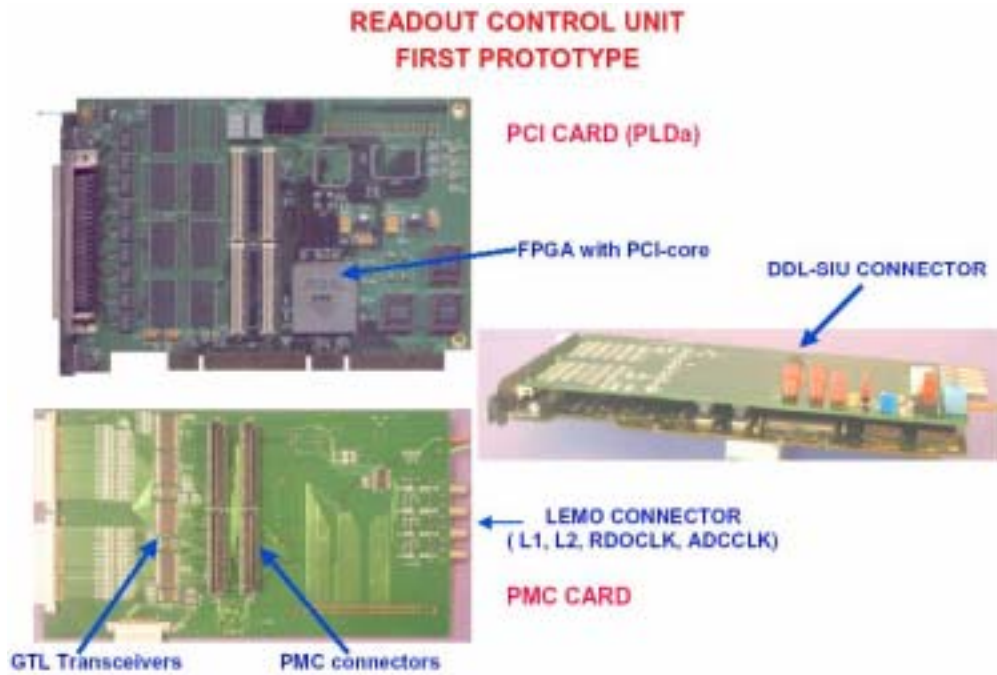


FIG. 27: Readout control unit PCI interface prototype[63]

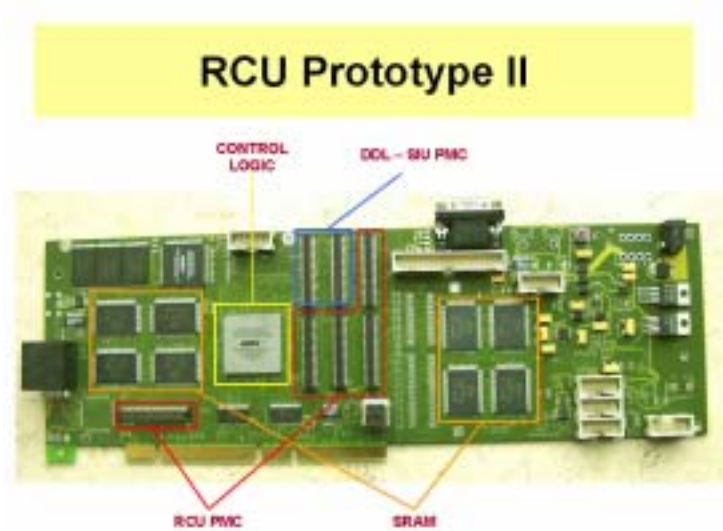


FIG. 28: Readout control unit alternate interface prototype[63]

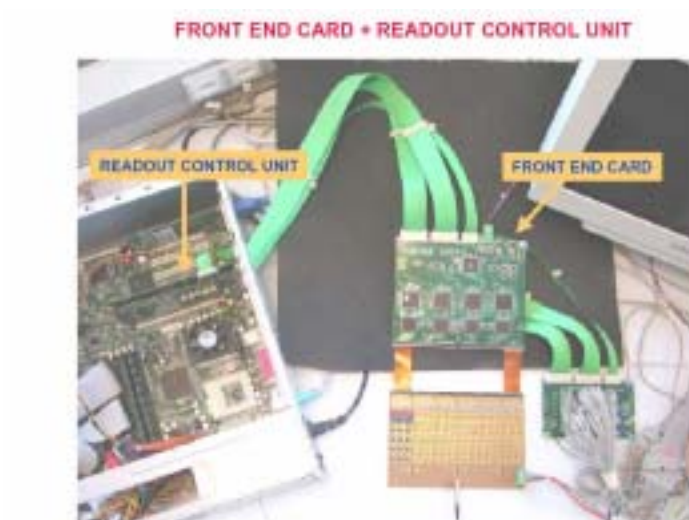


FIG. 29: Readout control unit test station[63]

bus at 20 MHz instead of the 40MHz design frequency. These modifications are projected to both increase stability and retain the utility of as much of the existing equipment as is possible.

The component requirements for the full system upgrade of the time projection chamber are listed in Table IV. The projected yield for the PASA and ALTRO wafers based upon the previous production run is estimated at 82%. When yield is included, it is estimated

that 1200 raw dies would be required to obtain enough components to instrument the detector.

The cost per channel for the ALTRO electronics solutions, dependent upon chip yield, is estimated at \$10 per channel based upon the electronics costs for instrumenting the BONUS TPC at Jefferson lab. The total cost of the front end electronics modifications is estimated at a direct cost of \$155,000 without contingency. Additional cost is incurred in the procurement of 10 single board VME style computers for event filtering and synchronization. Each single board processor is estimated to cost \$1800-2000 dependent upon final specifications and memory buffering requirements. The total cost of the VME processor boards is expected to be \$20k. The total direct cost of equipment for upgrading the E907 time projection chamber is estimated at \$175k without contingency.

The above cost estimates assume that the ALTRO and PASA chips needed by MIPP would be part of a larger production run. The next production run is slated to occur in May 2005. The testing and packaging of these chips would be done by institutions in the ALICE collaboration, who have developed custom test stands for verification of ALTRO and PASA chips. The amount needed for procurement of packaged and tested PASA and ALTRO chips is approximately \$105k.

XI. DATA COMPRESSION

The raw TPC output is in the form of waveforms in time for each pad. The data from the TPC can be compressed considerably by finding clusters and pulse-heights. This can be done by a modest farm of Level II processors, which can then bring down the data storage problem to manageable levels.

XII. UPGRADING THE REST OF THE MIPP DAQ TO RUN AT 3 KHZ

In order for the entire experiment to be able to read out at 3 kHz, a number of subsystems have to be upgraded for readout speed. Presently, MIPP is almost entirely relying on CAMAC electronics. In order to speed the DAQ rate, we would use more VME electronics, and FERA bus readout. Most of the necessary electronics is available from previous experiments; KTeV and HyperCP in particular. We note that several previous Fermilab

experiments (e.g E690, E771, E791), in addition to K-TeV and HyperCP have run at large event rates previously. MIPP is unique in having the TPC with a very large contribution to the event size. However, once the TPC DAQ rate is addressed, we expect the rest of the system to fall in line relatively easily.

The MIPP RICH detector has new VME electronics and can support required trigger rate. The hadronic calorimeter would not need to be upgraded either since it has few channels. Below are requirements for the rest of the subsystems and proposed ways to satisfy those requirements with minimal costs.

A. Electromagnetic Calorimeter

Presently, this is the slowest detector in terms of readout because it is relying on old ADC's. We can speed up the readout and still preserve the analog information by using LeCroy FERA ADC's which are available from Fermilab Electronics Equipment Pool.

B. Proportional Chambers

Number of Channels-5120 wires. The chambers are readout with RMH electronics which has a few problems associated with it

- It is unreliable, very difficult to debug
- Spare modules are hard to come by
- It cannot be driven at high rates because of the cable connecting preamps and discriminators

HyperCP has enough electronics for 20,000 channels of wire chambers. This is more than enough electronics for the 5,000 wires of the two proportional chambers.

C. Multicell Cerenkov

Number of Channels-96 The present readout of 96 TDC and ADC channels is unacceptably long for the upgrade. Readout speed would improve if FERA bus is used instead of standard CAMAC readout.

D. The Time of Flight system

Number of Channels- ≈ 100 . In order to make use of the time of flight wall, PMT signals must be timed with a TDC capable of 50 ps resolution or better. Readout of present electronics can be improved with zero suppression, but the electronics can only be readout through normal CAMAC. Readout time of charge on each PMT can be improved by using FERA bus.

E. Drift chambers

Number of Channels-7808 for drift chambers and 1920 wires for beam chambers. Both use same electronics. Drift chamber electronics consists of two physically separated parts: preamps and TDC's. Preamps are capable of being driven at very high rates. TDC's have unacceptably long digitization time, and at a rate of 1 kHz or above have readout errors. Therefore, it is necessary to upgrade both beam chambers and drift chambers.

CDF is retiring electronics that was used for central outer tracker. The 3000 channels that they can provide us will be sufficient to upgrade the three beam chambers. We will only have to build adapter boards to convert ECL signal output by discriminators to LVDS signal required by CDF boards.

F. Data Acquisition System Software

MIPP DAQ software is Linux based and resides in part on VME PowerPC's. MIPP uses a total of 6 VME computers to readout all electronics in parallel: 4 processors dedicated to TPC and 2 processors for the rest of the subsystems. Existing MIPP system was designed for operation in burst mode, that is when a 1 second spill would be delivered every 3 seconds. Data readout by VME PowerPC's is buffered until the end of a spill and then sent over 100 BaseT network to the server. The upgraded MIPP would be operating in a burst mode as well, so a significant part of the framework could be reused. In other words, it would not be necessary to go to a real time operating system like vxWorks.

In order to make the system reliable at 3 kHz readout rate, we would have to

- Improve interrupt handling

- Write better VME drivers
- Make use of DMA on the VME bus

All of these projects could be easily carried out by one or two people in a matter of 6 months.

XIII. COST AND WORK BREAKDOWN OF THE TPC ELECTRONICS UPGRADE

Table V gives the cost for the upgrade of the front end electronics of the TPC and the upgrade of the rest of the MIPP DAQ. In addition, we would like to fix one of the coils of the Jolly Green Giant, which has developed shorts.

A. Optional upgrades

It would be good to have the following subsystems in MIPP made more robust. It is not essential for successful running. The Cryogenic target is working on a refurbished cryocooler. A spare cryocooler would be a good investment. The TPC has broken several wires during our commissioning phase. It would be good to rewind the TPC from scratch and install new wires. Finally, MIPP lost several phototubes in the RICH during the fire. Replacing these would improve the RICH efficiency, although there is currently sufficient light for the RICH to function effectively. Tableoptup gives the cost breakdown of these optional upgrades. Table VII lists the manpower estimates for building the TPC electronics and table VIII lists the manpower estimates for fixing the Jolly green Giant coil.

XIV. RUNNING TIME NEEDED FOR THE PROPOSED PHYSICS FOR THE UPGRADED MIPP

Table IX gives the run times required for the physics topics proposed with the upgraded MIPP.

XV. CONCLUSIONS

We have proposed a low cost upgrade solution to the MIPP DAQ that will make MIPP a powerful spectrometer with hitherto unprecedented particle identification and acceptance and will permit the full dataset of our initial proposal to be obtained in a finite period of time. We have outlined other additional physics that can be done with such a device that will significantly enhance our knowledge of QCD.

-
- [1] See the MIPP proposal and addendum at <http://ppd.fnal.gov/experiments/e907/Proposal/P00-Proposal.pdf>
<http://ppd.fnal.gov/experiments/e907/Proposal/P01-Addendum.pdf>
 - [2] The rule imposed is that the fixed target SY120 program slow spills should not impose more than a 5% tax on the Tevatron luminosity.
 - [3] R. Raja, *Phys. Rev. D* **18**, 204 (1978).
 - [4] R. Raja, *Phys. Rev. D* **16**, 142 (1977).
 - [5] J. Lenz, Private Communication.
 - [6] G. Rai et al., *IEEE Trans. Nucl. Sci.* **37**, 56 (1990).
 - [7] L. Musa, et al., *IEEE NSS* Oct 2003.
 - [8] R.Raja, Y.Fisyak in Proceedings of the DPF92 meeting, Fermilab.
 - [9] G.C. Rossi and G. Veneziano *et al.*, *Nucl. Phys.* B123:507 (1977)
 - [10] S. Vance and M. Gyulassy *et al.*, *Phys. Rev. Lett.*83:1735 (1999)
 - [11] F. Antinori *et al.*, *Phys. Lett.* B449:401 (1999)
 - [12] M.M. Aggarwal *et al.*, *Eur. Phys. G.* C18:651 (2001)
 - [13] W. Busza *et al.*, *Phys. Rev. Lett.* 34:836 (1975)
 - [14] I. Chemakin *et al.*, *Phys. Rev. Lett.* 85:4868 (2000)
 - [15] I. Chemakin *et al.*, *Phys. Rev. C* 60:024902 (1999)
 - [16] L. Van Hove,*Z. Phys. C* **9**, 145 (1981).
 - [17] K. Adcox *et al.*, *Phys. Rev. Lett.*86:3500 (2001)
 - [18] D. Kharzeev and M. Nardi *et al.*, *Phys. Lett.* B507:121 (2001)
 - [19] H. Atherton *et al.*, **CERN 80-07**, (1980).
D. Barton *et al.*,*Phy.Rev.* **27** (1983) 2580.

- G. Ambrosini *et al.*(SPY collaboration), Phys. Lett. **B420** (1998)225;Phys. Lett. **B425** 208;, Eur. Phys. J. **C10**(1999) 605.
- [20] R. Brun, F. Bruyant, A. C. McPherson, P. Zancarini, CERN Data handling Division, (Geant3), DD/EE/84-1, 1987; CERN Program Library, W5103(1994).
M. Bonesini, A. Marchionni, F. Pietropaolo and T. Tabarelli de Fatis,(BMPT) Eur.J.Phys C, DOI 10.1007/S100520100656 (hep-ph/0101163).
N. V. Mokhov and S. I. Strihganov, “Model for Pion Production in Proton-Nucleus Interaction” AIP Conf. proc. **435** 91997) 543. N.V.Mokhov, The MARS Code System User’s Guide, version 13(95), Report Fermilab-FN-628(1995); <http://www-ap.fnal.gov/MARS>.
A. J. Malensek, Fermilab-FN 341, (1981).
- [21] The SAID partial-wave analysis facility is online at <http://gwdac.phys.gwu.edu/>.
- [22] D. M. Manley, R. A. Arndt, Y. Goradia, and V. L. Teplitz, Phys. Rev. D **30**, 904 (1984).
- [23] S. Prakhov *et al.* (Crystall Ball Collaboration), Phys. Rev. C **69**, 045202 (2004).
- [24] M. Ripani *et al.* (CLAS Collaboration), Phys. Rev. Lett. **91**, 022002 (2003).
- [25] *Review of Particle Physics*, S. Eidelman *et al.* (Particle Data Group), Phys. Lett. B **592** 1, (2004).
- [26] Bertanza *et al.*, Phys. Rev. Lett. **8**, 332 (1962).
- [27] Knasel *et al.*, Phys. Rev. D **11**, 1 (1975).
- [28] Binford *et al.*, Phys. Rev. **183**, 1134 (1969).
- [29] Saxon *et al.*, Nucl. Phys. **B162**, 522 (1980).
- [30] Van Dyke *et al.*, Phys. Rev. Lett. **23**, 50 (1969).
- [31] Dahl *et al.*, Phys. Rev. **163**, 1430 (1967).
- [32] Jones *et al.*, Phys. Rev. Lett. **26**, 860 (1971).
- [33] M. Q. Tran *et al.* (SAPHIR Collaboration), Phys. Lett. B **445** 20 (1998).
- [34] T. Mart and C. Bennhold, Phys. Rev. C **61**, 012201 (1999).
- [35] J. McNabb *et al.* (CLAS Collaboration), Phys. Rev. C **69** (2004) 042201.
- [36] A. Salam, K. Miyagawa, H. Arenhoevel, T. Mart, C. Bennhold and W. Gloeckle, nucl-th/0411036.
- [37] R. Erbe *et al.* Phys. Rev. **188** 2060 (1969).
- [38] S. Capstick and W. Roberts, Phys. Rev. D **58**, 074011 (1998).
- [39] Grether *et al.*, Phys. Rev. D **7**, 3200 (1973).

- [40] Abolins *et al.*, Phys. Rev. Lett. **11**, 381 (1963).
- [41] Abrams *et al.*, Phys. Rev. Lett. **25**, 617 (1970).
- [42] Alff *et al.*, Phys. Rev. **145**, 1072 (1966).
- [43] Brown *et al.*, Phys. Rev. Lett. **19**, 664 (1967).
- [44] Chapman *et al.*, Phys. Rev. D **3**, 38 (1971).
- [45] Trilling *et al.*, Phys. Lett. **19**, 427 (1965).
- [46] Yamamoto *et al.*, Phys. Rev. **140**, 730 (1965).
- [47] Buhl *et al.*, Phys. Lett. **48B**, 388 (1974).
- [48] Pohls *et al.*, Nucl. Phys. **B25**, 109 (1971).
- [49] S. Capstick and W. Roberts, Phys. Rev. D **57**, 4301 (1998).
- [50] A. R. Dzierba, C. A. Meyer and A. P. Szczepaniak, arXiv:hep-ex/0412077, (2004).
- [51] J. Napolitano, J. Cummings and M. Witkowski, arXiv:hep-ex/0412031, (2004).
- [52] J. Pochodzalla, arXiv:hep-ex/0406077, (2004).
- [53] K. Hicks, arXiv:hep-ex/0412048, (2004).
- [54] J. W. Price *et al.*, arXiv:nucl-ex/0402006, (2003).
- [55] J. W. Price *et al.* (CLAS Collaboration), arXiv:nucl-ex/0409030, (2004), and accepted for publication in Phys. Rev. C.
- [56] Alt C *et al.* (NA49 Collaboration), Phys. Rev. Lett. **92**, 042003-1 (2004).
- [57] PLD Applications, <http://www.plda.com>
- [58] B. Mota, L.Musa , R. Esteve and A. Jimenez de Parga, in *Proc. of the 6th Workshop on Electronics for LHC Experiments* (2000).
- [59] D. Subiela, S. Engels and L. Dugoujou, in *Proceedings of the ESSCIRC, 28th European Solid State Circuits Conference*, (2002).
- [60] L. Musa et al., in *Proc. of the IEEE Nuclear Science Symposium* (2003).
- [61] R. Bosch,A. Parga,B. Mota, and L. Musa, IEEE Trans. Nucl.Sci. 50 (2003).
- [62] R. Campagnolo et.al., in it Proceedings of the 9th workshop on Electronics for LHC Experiments (2003).
- [63] R. Bosch et.al., in *Proceedings of the 8th Workshop on Electronics for LHC Experiments* (2002).

Summary (million events)			Beam Momentum (GeV/c)										Grand	
Priority	Target	Note	5	13.3	15	20	30	40	50	60	75	120	Total	
1	H		1.00		0.80				1.80		1.80		5.40	
	Be	p only										1.00	1.00	
									0.50				0.50	
	C	p only	0.38				0.38					0.38	1.14	
	Bi	p only										0.38	0.38	
						0.50			1.00					1.50
	U								1.00					1.00
NuMI	p only											0.38	0.38	
1 Total			1.00	0.38	0.80		0.50	0.38	4.30		1.80	2.76	11.92	
2	H		1.40		0.40		1.40		0.40		0.40		4.00	
	D		0.30		0.30		0.30		0.30		0.30		1.50	
	Be	p only										2.00	2.00	
							1.00		0.50				1.50	
	N		0.50	0.50			0.50						1.50	
	C	p only				0.29			0.29			0.58	1.16	
	Bi	p only										2.00	2.00	
						0.50			1.00		1.00		2.50	
U								1.00				1.00		
NuMI	p only											1.15	1.15	
2 Total			2.20	0.50	0.70	0.29	3.70		3.20	0.29	1.70	5.73	18.31	
3	H		3.00		3.00		3.00		3.00		3.00		15.00	
	D		0.30		0.30		0.30		0.30		0.30		1.50	
	Be	p only										3.00	3.00	
		2× tgt										0.60	0.60	
			1.00	1.00					0.81		1.00		3.81	
	N		0.50	0.50			0.50						1.50	
	C	p only	0.62		0.62		0.62		0.62		0.62		3.10	
			1.00										1.00	
		pi,K only			0.66		0.66		0.66				1.98	
	Cu						1.00		2.00		1.00		4.00	
												4.00		
Bi	p only										3.00	3.00		
	2× tgt										0.60	0.60		
		1.00	1.00									2.00		
NuMI	p only											3.08	3.08	
3 Total			6.80	3.12	3.30	1.28	4.80	1.28	6.11	1.28	5.30	14.90	48.17	
Grand Total			10.00	4.00	4.80	1.57	9.00	1.66	13.61	1.57	8.80	2.39	78.40	

TABLE I: MIPP run plan summary. The units are in millions of events on various targets.

Momentum GeV/c	p	K^+	π^+	\bar{p}	K^-	π^-
1	5752	0	64798	7907	0	30425
2	23373	194	459718	26863	142	236494
3	53431	3060	1069523	51424	2221	598742
5	153220	32763	2400799	103996	23164	1550810
10	663916	223210	5006708	195767	142777	3862225
15	1618120	443557	7141481	221602	245868	5248463
20	3113387	655426	9290219	212171	306685	5841030
30	8158054	1043430	12770579	160329	340144	5837467
40	16664431	1294189	13944272	101617	288728	5156862
50	29288928	1338452	12788523	53056	196400	4114582
60	45985629	1191744	10094311	22092	108032	2905091
70	65227010	919279	6834097	6987	47093	1762060

TABLE II: Secondary beam fluxes as a function of beam momentum and species for 2E11 primary protons on target

TABLE III: Momentum bins for π^\pm running, and corresponding c.m. energy W . Also given is the amount of beam time that would be desirable at each momentum. . The lowest beam momentum bins can probably be done with far fewer hours with an improved beam line.

p_{lab}	W	Time π^+	Time π^-	p_{lab}	W	Time π^+	Time π^-
(GeV/c)	(GeV)	(Hours)	(Hours)	(GeV/c)	(GeV)	(Hours)	(Hours)
0.80	1.557	170	124	1.55	1.955	22	32
0.85	1.586	109	76	1.60	1.978	21	29
0.90	1.615	106	54	1.65	2.002	20	27
0.95	1.644	78	41	1.70	2.025	19	25
1.00	1.672	61	32	1.75	2.048	18	23
1.05	1.699	50	27	1.80	2.071	18	22
1.10	1.726	42	22	1.85	2.093	18	22
1.15	1.753	36	19	1.90	2.115	17	22
1.20	1.780	31	17	1.95	2.137	17	22
1.25	1.806	27	15	2.00	2.159	17	22
1.30	1.831	25	15	2.10	2.202	17	23
1.35	1.857	23	15	2.20	2.244	18	23
1.40	1.881	24	17	2.30	2.286	18	23
1.45	1.906	24	19	2.40	2.326	19	23
1.50	1.930	23	23	2.50	2.366	20	24

Component	Channels	no. Per FEC	Total Required
Front End Circuit Board	120	1	128
ZIF Sockets		1	128
Preamp/Shaper (PASA)	16	8	960
ADC/Filter/Memory (ALTRO)	16	8	960
Readout Control Units (RCU)	1536	1:12	10
Single Board VME PCs	1536	1:12	10
PCI Mezzanine Receivers	1536	1:12	10
Gigabit Network Switch			1

TABLE IV: Component requirements for upgrade of the E907 time projection chamber for operation at 3kHz.

Acquire 1100 ALICE Altro/Pasa chips (tested at Lund) (Needed May 2005)	\$105,000
Cost of other items in table IV	\$50,000
TPC total Front end electronics cost	\$155,000
VME processor boards	\$20,000
Test stand	\$30,000
Total TPC electronics upgrade cost	\$205,000
Contingency (10%)	\$20,500
Total TPC electronic upgrade cost	\$222,500
Cost to upgrade the rest of the MIPP DAQ	\$50,000
Total DAQ upgrade cost	\$275,500
Jolly Green Giant Coil Fix	\$145,000
Total	\$420,000

TABLE V: Cost Breakdown for TPC electronics upgrade

Cryogenic target -Extra cryo cooler	\$32,000
TPC Rewind (M&S)	\$10,000
RICH phototube upgrade (Hamamatsu tubes, bases)	\$204,000

TABLE VI: Cost Breakdown for optional upgrades

Job	Time	Person
Writing FPGA code for both boards	1 month	engineer
Design front end circuit board	1 month	engineer
Layout	3 weeks	electrical drafting group
Assembly of prototype	1 week	technician
Debug/testing of prototype	3 weeks	engineer/technician
Design controller board(s)	1 month	engineer
Layout	1 month	electrical drafting group
Assembly of prototype	1 week	technician
Debug/testing of prototype	1 month	engineer/technician
Design of test injection card	1 week	engineer
Layout	1 week	electrical drafting group
Assembly of test card	1 week	technician
Debug/testing of card	1 week	engineer
Software for test stand	1 month	software engineer (or physicist?)
Running production tests on front boards	2 weeks	engineer/technician
repair of failed front end boards	2-4 weeks	technician
Testing readout controllers	1 week	technician
repairing failed controller boards	1 week	technician
oversight of entire procurement process	2 weeks	technician
parts, contract assembly etc.		
Document preparation, updating	2 weeks	engineer/technician

TABLE VII: Manpower break down for building the TPC Front end electronics cards

Equipment	Action	Manpower	Manweeks	M&S
BCKOV	secure & disconnect vacuum	2 techs, 2 weeks	4	
	re-install vacuum & test	3 techs, 3 weeks	9	
	remove cable tray & hardline	2 techs, 1 week	2	
	re-install cable tray & hardline	3 techs, 2 weeks	6	
	M&S purchases	\$2K		\$2,000
Beam pipe & concrete supports	move to side	4 techs, 1 week	4	
	re-install	4 techs, 2 weeks	8	
LH2 Target	Move LH2 target equipment out	2techs 1 week	2	
TPC	De-cable	By experimenters		
	Re-cable	By experimenters		
	remove electrical conduit	M&S \$4K		\$4,000
	re-install electricalconduit	M&S \$8K		\$8,000
	move out TPC & support stand	3 techs, 1 week	3	
	re-install TPC & support stand	3 techs, 1 week	3	
JGG	de-cable	2 techs, 2 days		
	re-cable	2 techs, 3 days	1	
	de-hose	1 tech, 1 day		
	re-hose	1 tech, 4 days	1	
	remove coil	M&S \$15K	1	\$15,000
	install coil	M&S \$6K	1	\$6,000
Repair JGG coil	M&S	\$90K		\$90,000
	OH	\$20K		\$20,000
	total man-weeks		45	
	total M&S			\$145,000

TABLE VIII: Manpower break down for moving the TPC and fixing the Jolly Green Giant Coil

Physics Topic	Run Time (days)
MIPP -I	18.1 days
New neutrino experiment target (10^7 events)	2.3 days
Additional Nucleus (<i>5millionevents</i>)	1.15 days
Two particle inclusive scaling (100 million events)	23.1 days
Pentaquark search (K^+ beam)	12 days
Cascades search (K^- beam)	15 days
Missing baryon search using low momentum pions	82 days

TABLE IX: Run times required per physics topic assuming a single 4 second spill every two minutes and a 50% duty factor for delivering beam.